

Factors modifying cellular response to ionizing radiation

Lei Cheng



Factors modifying cellular response to ionizing radiation

Lei Cheng

Academic dissertation for the Degree of Doctor of Philosophy in Molecular Bioscience at Stockholm University to be publicly defended on Wednesday 5 June 2019 at 13.00 in P216, NPQ-huset, Svante Arrhenius väg 20.

Abstract

Many physical factors influence the biological effect of exposure to ionizing radiation, including radiation quality, dose rate and temperature. This thesis focuses on how these factors influence the outcome of exposure and the mechanisms behind the cellular response.

Mixed beam exposure, which is the combination of different ionizing radiations, occurs in many situations and the effects are important to understand for radiation protection and effect prediction. Recently, studies show that the effect of simultaneous irradiation with different qualities is greater than simple additivity of single radiation types, which is called a synergistic effect. But its mechanism is unclear. In **Paper I, II** and **III**, alpha particles and X-rays were used to study the effect of mixed beams. **Paper I** shows that mixed exposure induced a synergistic effect in generating double strand breaks (DSB), and these DSB were repaired by slow kinetics in U2OS cells. In **Paper II**, alkaline comet assay was applied to investigate the induction and repair of DNA lesions including DSB, single strand breaks and alkali labile sites in peripheral blood lymphocytes (PBL). We demonstrate that mixed beams interact in inducing DNA damage and influencing DNA damage response (DDR), which result in a delay of DNA repair. Both in **Paper I** and **II**, mixed beams showed a capability in inducing higher activity of DDR proteins than expected from additivity. **Paper III** investigates selected DDR-related gene expression levels after exposure to mixed beams in PBL from 4 donors. Synergy was present for all donors but the results suggested individual variability in the response to mixed beams, most likely due to life style changes.

Low temperature at exposure is radioprotective at the level of cytogenetic damage. In **Paper IV**, data indicate that this effect is through promotion of DNA repair, which leads to reduced transformation of DNA damage into chromosomal aberrations.

Paper V aims to compare the biological effectiveness of gamma radiation delivered at a very high dose rate (VHDR) with that of a high dose rate (HDR) in order to optimize chronic exposure risk prediction based on the data of atomic bomb survivors. The results suggest that VHDR gamma radiation is more effective in inducing DNA damage than HDR.

Keywords: *Radiation biology, DNA damage, gene expression, alpha particles, X-rays, mixed beams, gamma rays, hypothermia, dose rate.*

Stockholm 2019

<http://urn.kb.se/resolve?urn=urn:nbn:se:su:diva-168023>

ISBN 978-91-7797-725-4
ISBN 978-91-7797-726-1



Department of Molecular Biosciences, The Wenner-Gren Institute

Stockholm University

Stockholm University, 106 91 Stockholm

FACTORS MODIFYING CELLULAR RESPONSE TO IONIZING
RADIATION

Lei Cheng



Factors modifying cellular response to ionizing radiation

Lei Cheng

©Lei Cheng, Stockholm University 2019

ISBN print 978-91-7797-725-4

ISBN PDF 978-91-7797-726-1

Printed in Sweden by Universitetservice US-AB, Stockholm 2019

To my family

Populärvetenskaplig sammanfattning

Joniserande strålning är en naturlig del av våra liv, vår omgivning och våra kroppar. Strålning är även ett vanligt kliniskt verktyg, främst vid diagnostik och cancerbehandling. Det finns två huvudtyper av joniserande strålning, elektromagnetisk strålning och partikelstrålning. Båda dessa stråltyper kan skada DNA-baser samt bryta den ena eller båda DNA-strängarna, vilket kan leda till mutationer och i värsta fall cancer. Celler, vävnader och organismer reagerar på olika sätt mot strålning och det finns flera faktorer som påverkar reaktionen. Faktorerna inkluderar biologiska och fysikaliska aspekter. Biologiska aspekter beror på cellernas genetiska bakgrund och modifiering av cellens respons via miljöfaktorer. Fysikaliska aspekter inkluderar strålslaget, dosen och strålningens doshastighet. För att kunna vara säker på att nuvarande strålskyddssystem är tillräckligt bra, är det mycket viktigt att studera faktorer som kan påverka den cellulära responsen vid exponering för strålning.

Avhandlingens första del fokuserar på strålslaget. Även om det finns många studier om cellulära effekter av strålning av olika slag, så saknas det fortfarande kunskap om cellers reaktion mot blandat fält av tätt och glest joniserande strålning. Blandad strålning inträffar när båda dessa stråltyper finns närvarande samtidigt, t.ex. när bakgrundsstrålningen inkluderar radon, vid exponering för kosmisk strålning under flygresor samt vid vissa former av cancerbehandling. Den stora frågan är om de två typerna interagerar och därmed inducerar en synergistisk effekt. Vad är mekanismen för interaktionen?

I **manuskript I** användes U2OS celler som uttrycker ett fluorescensmarkerat DNA reparationsprotein kallat 53BP1. 53BP1 bildar så kallade foci kring DNA dubbelsträngbrott (DSB). Resultaten visar att alfa- och röntgenstrålning interagerar och utlöser en högre nivå av DSB än förväntat. DSB som inducerades av blandat fält var komplexa och cellerna reparerade dem långsammare än DSB som inducerades av alfa- eller röntgenstrålning var för sig. I **manuskript II** användes en annan metod och en annan celltyp för att studera effekten av blandat fält. Med hjälp av den så kallade kometmetoden (eller single cell gel electrophoresis) som samtidigt mäter nivån av flera typer av DNA skador kunde vi visa att blandad strålning utlöser komplexa skador även i

mänskliga lymfocyter. Liksom i U2OS celler reparerade lymfocyterna skadorna långsammare än dem som inducerades av alfa och röntgenstrålning var för sig. Dessutom fanns en tydlig effekt av blandat fält på nivån av aktivering av DNA reparationsproteiner. Detta resultat gav anledning att studera vidare hur blandat fält påverkar reglering av genuttryck i lymfocyter.

I **manuskript III** användes qPCR-tekniken (quantitative real time polymerase chain reaction) för att analysera mRNA nivåer av 6 gener som induceras av DNA skador. Analysen genomfördes i lymfocyter från 4 donatorer. I tre av dem var mRNA-nivån konsekvent högst i cellerna som exponerats med blandat fält. I lymfocyter från den fjärde donatorn var resultatet variabelt, troligen på grund av förändringar i livsstilen.

I **manuskript IV** undersökte vi en hypotes kring mekanismen bakom den strålskyddande effekten av hypotermi. Temperaturen vid bestrålning kan påverka den biologiska effekten av strålning, och man ser oftast att en lägre temperatur vid bestrålningen leder till en lägre nivå av kromosomala skador. Med hjälp av PCC (premature chromosome condensation) tekniken undersökte vi omvandlingskinetiken från primära kromosomala skador (PCC breaks) till kromosomala avvikelser i mänskliga lymfocyter. Lymfocyter bestrålades i isvatten eller vid 37 °C. Resultaten visar att den strålskyddande effekten av hypotermi syns omedelbart efter bestrålning, alltså på nivå av primära kromosomala skador.

Cellulära effekter av de låga doshastigheter som finns i områden med hög naturlig bakgrundsstrålning är relativt välstuderade. Däremot finns få studier om effekter av väldigt de höga doshastigheter som uppstår när en atombomb exploderar. Syftet med **manuskript V** var att analysera effekten av hög doshastighet på genuttryck och bildning av mikrokärnor i mänskliga lymfocyter. Cellerna bestrålades med olika doser och tre doshastigheter: 0,4, 0,8 och 8,0 Gy/min. Resultaten visar att antalet DNA skador per dosenehet är högst vid den väldigt höga doshastigheten 8 Gy/min. Resultaten bekräftades i U2OS cellerna.

List of publications

This thesis is based on the following publications/manuscripts:

- I. Sollazzo A, Brzozowska B, **Cheng L**, Lundholm L, Haghdoost S, Scherthan H, & Wojcik, A. *Alpha Particles and X Rays Interact in Inducing DNA Damage in U2OS Cells*. Radiation Research. 2017;188(4):400-11.
- II. **Cheng L**, Lisowska H, Brzozowska B, Sollazzo A, Lundholm L, Lisowska H, Haghdoost S, & Wojcik A. *Simultaneous induction of dispersed and clustered DNA lesions compromises DNA damage response in human peripheral blood lymphocytes*. PLoS One. 2018;13(10):e0204068.
- III. **Cheng L**, Brzozowska B, Wojcik A, Lundholm L. *Impact of ATM and DNA-PK inhibition on gene expression and individual response of human lymphocytes to mixed beams of alpha particles and X-rays*. Manuscript.
- IV. Lisowska H, **Cheng L**, Sollazzo A, Lundholm L, Wegierek-Ciuk A, Sommer S, Lankoff A, & Wojcik A. *Hypothermia modulates the DNA damage response to ionizing radiation in human peripheral blood lymphocytes*. International Journal of Radiation Biology. 2018; 94(6):551-7.
- V. Olofsson D, **Cheng L**, Fernández R B, Lipka M, Riego M L, Akuwudike P, Lisowska H, Lundholm L, Wojcik A. *Biological effectiveness of very high gamma dose rate and its implication for radiological protection*. Manuscript.

Paper I, II and IV are reproduced with permission from the publishers.

Papers not included in this thesis

- **Cheng L**, Lisowska H, Sollazzo A, Wegierek-Ciuk A, Stepień K, Kuszewski T, Lankoff A, Haghdoost S, Wojcik A. *Modulation of radiation-induced cytogenetic damage in human peripheral blood lymphocytes by hypothermia*. Mutation Research. Genetic Toxicology and Environmental Mutagenesis. 2015;793:96-100.
- Brzozowska B, Sollazzo A, **Cheng L**, Lundholm L, Wojcik A. *EP-2072: Spatiotemporal dynamics of DNA damage in cells exposed to mixed beams of ionising radiation*. Radiotherapy and Oncology. 2016;119:977-978
- Sollazzo A, Brzozowska B, **Cheng L**, Lundholm L, Scherthan H, Wojcik A. *Live Dynamics of 53BP1 Foci Following Simultaneous Induction of Clustered and Dispersed DNA Damage in U2OS Cells*. International Journal of Molecular Sciences. 2018;19(2)
- Gałecki M, Tartas A, Szymanek A, Sims E, Lundholm L, Sollazzo A, **Cheng L**, Fujishima Y, Yoshida M A, Żygierewicz J, Wojcik A, Brzozowska-Wardecka B. *Precision of scoring radiation-induced chromosomal aberrations and micronuclei by unexperienced scorers*. International Journal of Radiation Biology. 2019. In press.

Contents

Sammanfattning.....	i
List of publications.....	iii
Papers not included in this thesis.....	iv
Contents.....	v
Abbreviations.....	vii
Introduction.....	1
Radiation.....	1
Linear energy transfer.....	2
Relative biological effectiveness.....	3
Direct and indirect effect.....	3
Radiation-induced DNA damage.....	4
DNA damage response.....	5
Repair pathways after DNA damage.....	6
Proteins involved in DDR.....	8
Radiation-related genes.....	9
Factors which modulate the biological effects of radiation.....	10
Mixed beam effect.....	10
Temperature effect at radiation exposure.....	11
Dose rate.....	12
Aims.....	15
Material and Methods.....	16
U2OS cell line and 53BP1 foci.....	16
Blood.....	16

Irradiation.....17
Western blot.....18
Comet assay.....18
The cytokinesis-block micronuclei assay.....19
Quantitative PCR.....20
Premature chromosome condensation.....20
Envelope analysis.....21
Results and Discussion.....22
 Paper I.....22
 Paper II.....25
 Paper III.....27
 Paper IV.....30
 Paper V.....32
Conclusions and future studies.....35
Acknowledgements.....37
References.....39

Abbreviations

·OH	Hydroxyl radicals
alt-NHEJ	Alternative NHEJ
ATM	Ataxia-telangiectasia mutated
BAX	Bcl-2-associated X protein
BER/SSBR	Base excision repair/single-strand break repair
BNC	Binucleated cells
bp	Base pairs
BRCA1	Breast cancer type 1 susceptibility protein
CBMN	Cytokinesis-block micronuclei
CDC25A	Cell division cycle 25A
CDK2	Cyclin-dependent kinase 2
CDKN1A	Cdk inhibitor p21
Chk2	Checkpoint kinase 2
Ct	Cycle threshold
Cyt-B	Cytochalasin-B
DDR	DNA damage response
DREF	Dose Rate Effectiveness Factor
DNA-PKcs	DNA-dependent protein kinase catalytic subunit
DSB	Double-strand break
Endo III	Endonuclease III
FAT	FRAP-ATM-TRRAP
FDXR	Ferredoxin reductase
Fpg	Formamidopyrimidine [fapy]-DNA glycosylase
GADD45a	Growth arrest and DNA damage inducible alpha
GAPDH	Glyceraldehyde-3-phosphate dehydrogenase
HDR	High dose rate
HR	Homologous recombination

HZE	High Z number elements
ICRP	International Committee on Radiological Protection
IR	Ionizing radiation
IRIF	Ionizing radiation induced repair foci
Ku70/Ku80	70/80 kDa subunit of Ku antigen or XRCC6/5
LDR	Low dose rate
LET	Linear energy transfer
LF	Large foci
LSS	Life span study
MDM2	Mouse double minute 2 homolog
MMEJ	Microhomology-mediated end-joining
MN	Micronuclei
MRN	Mre11-Rad50-Nbs1 complex
NER	Nucleotide excision repair
NHEJ	Non-homologous end joining
p53	TP53, cellular tumour antigen p53
PBL	Peripheral blood lymphocytes
PCC	Premature chromosome condensation
PCCs	Prematurely condensed chromosomes
PP4C	Protein phosphatase 4C
qPCR	Quantitative polymerase chain reaction
RAD50	Radiation sensitive 50
RAD51	Radiation sensitive 51
RAD9	Radiation sensitive 9
RBE	Relative biological effectiveness
RIF	Radiation-induced foci
RPA	Replication protein A
RT	Room temperature
RTI	Relative tail intensity
SF	Small foci
SSB	Single-strand break
TE	Temperature effect
TEM	Transmission electron microscopy
TK6	Thymidine kinase heterozygote cell line
TSA	Trichostatin A

UNSCEAR	United Nations Scientific Committee on the Effects of Atomic Radiation
VHDR	Very high dose rate
XLF	XRCC4-like factor
XPC	Xeroderma pigmentosum, complementation group C
XRCC4	X-ray repair cross-complementing protein 4
γ H2AX	Phosphorylated H2AX at serine-139

Introduction

Radiation

Radiation is a kind of energy travelling through space or matter in the form of waves or particles. X-rays and γ -rays can be both described as waves and particles (photons). Particle radiation is composed of high energy sub-atomic particles, including alpha particles (helium-4 nuclei), beta particles (high-speed electrons or positrons), neutrons, protons and high Z number elements (HZE). Radiation is usually categorized into two types, ionizing radiation (IR) or non-ionizing radiation, according to its ability to induce ionization. If the energy of radiation is high enough to eject one or more orbital electrons from an atom or molecule, the radiation is called ionizing radiation. If the absorbed energy is not high enough to ionize but only cause excitation of atoms or electrons, that radiation is called non-ionizing radiation. IR include X-rays, γ -rays, α particles, β particles, neutrons, protons and HZE. Radio waves, radiant heat, visible light, ultraviolet light in the UVB and UVC range as well as microwaves are non-ionizing radiations (1). Since X-rays were discovered in 1895, the technique of radiation is increasingly applied in many branches of science, industry, medicine and in normal life, such as medical diagnosis and treatment, nuclear power and industrial radiography. Radiation does not only have benefits but also carries risks and dangers. IR is much more harmful than non-ionizing radiation to cells and live organisms as it can induce ionizations and change cell structures, and it is extensively studied. Radiobiology is defined as “the study of the action of ionizing radiations on living things” (2). The present study focuses on two types of IR: X-rays and alpha particles.

IR exists naturally everywhere, generated from decay of radioactive elements in the environment and in our bodies, or produced from interaction of cosmic rays with Earth’s atmosphere, which is called secondary cosmic rays (3). IR which is used artificially may also be emitted in the process of natural decay of some unstable nuclei or following excitation of atoms and their nuclei in nuclear reactors, cyclotrons, X-ray machines or other instruments (4). In this study, X-rays were generated from an X-ray tube that converts electrical

power into photons, while alpha particles were from α -decay of an ^{241}Am source, which has a half-life of 432.2 years, making the alpha source very stable with respect to the dose rate. Unlike gamma rays or electromagnetic waves as X-rays, alpha particles are positively charged and have a low penetration depth. They can be stopped by a sheet of paper, by a few centimeters of air or by the skin. Alpha particles can only penetrate about 0.05 mm of water and soft tissue. Alpha particles, protons and other ion particles lose most of their energy at the end of the track before stopping, which means that a pronounced peak in ionization density induced towards the end of their tracks. This kind of energy-loss curve is called Bragg curve and is well used in the cancer therapy (2).

Linear energy transfer

If energy of IR is absorbed by matter, ionizations and excitations occur along the tracks of the particles according to the type of radiations. This energy deposition process is assumed to be progressive and continuous. Linear energy transfer (LET) is defined as the energy transferred per unit length of the track. The unit of LET is $\text{keV}/\mu\text{m}$ and it depends on the types of IR and the material traversed. LET is an average quantity, as the energy deposition along the track per unit length varies over a wide range at the microscopy level (2). Generally speaking, it can be stated that, the LET value is directly related to energy of the ionization particle and stopping power. For practical reasons, IR is divided into low and high LET with the threshold of $10 \text{ keV}/\mu\text{m}$.

Low LET radiations include electrons and photons, which induce sparsely distributed ionizations and excitations in a large targeted volume. Typical values of low LET IR are around $0.2 \text{ keV}/\mu\text{m}$ for cobalt-60 gamma rays or a few $\text{keV}/\mu\text{m}$ for X-rays. High LET radiations include alpha particles, neutrons (where the LET is related to recoil protons) and HZE. As these particles have very much higher weight compared to an electron or photon, deflection of the particles will not occur and the tracks are almost linear and short. The LET of these radiations is higher than $10 \text{ keV}/\mu\text{m}$, for example, $166 \text{ keV}/\mu\text{m}$ for 2.5-MeV alpha particles. The ionizations and excitations induced by high LET are densely distributed around the track and can induce clustered DNA damages which are difficult to repair. Usually, high LET IR can induce higher biological effectiveness compared to low LET (2, 5).

Relative biological effectiveness

The quantity of IR is described as absorbed dose, which represents the amount of energy absorbed per unit mass. The unit is gray (Gy) where $1 \text{ Gy} = 1 \text{ J/kg}$. The same dose of different types of IR usually induce unequal biological effects. For example, high LET can induce greater biological effect than low LET, as the number of clustered DNA damage and the degree of their complexity were increased with LET (6, 7). Then a special parameter, relative biological effectiveness (RBE), is applied to evaluate the difference, specifically in relation to their cancer-producing effects. RBE is the ratio of the absorbed dose of a reference radiation to the absorbed dose of a test radiation when causing the same level of biological effect in a certain biological system (8). Low LET radiations are used as the reference radiations for calculating RBE. It was found that RBE increased with LET until it reaches a maximum value at ca $100 \text{ keV}/\mu\text{m}$ by clonogenic cell survival assay. They explained as radiations with this density of energy transferred to DNA have the highest probability to cause double-strand breaks (DSB), which means the average distance of the two ionizations is the diameter of the DNA double helix (2, 9). But actually, RBE values vary in different test systems. RBE is not only influenced by LET, but also depends on radiation dose, number of dose fractions, dose rate, biological system and endpoint (2). Because of a curvilinear response at higher acute doses of the reference low LET radiation, RBE of high LET increases to a maximum value at low dose and dose rate (8).

Direct and indirect effect

IR has two ways to induce damage in a target such as DNA, referred to as direct effect and indirect effect (Figure 1). Direct effect is when radiation particles interact directly with the DNA molecules, the critical cellular target, through ionizations and excitations to disrupt the molecular structure. This process is predominant with high LET radiation and at high radiation doses. In the indirect effect, radiation induces radiolysis first by hitting the water molecules which are the major constituent of cells. Then the water radiolysis products, free radicals and hydrogen peroxide, can react with the nearby ($< 4 \text{ nm}$) target molecules. Indirect effect is thought to be the major way of low LET radiation-induced DNA damage (5, 10).

Radiation-induced DNA damage

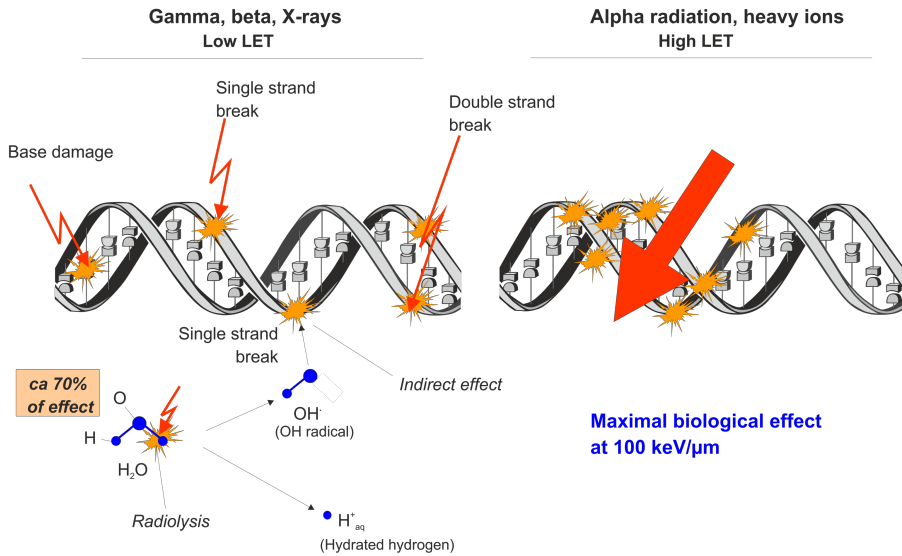


Figure 1. Radiation-induced DNA damage and the difference between high LET and low LET radiation

Radiation-induced DNA damage

IR can damage all important components of the cell, ranging from lipids to proteins or DNA. Among all, DNA is thought to be the main target of IR inside a cell. The types of DNA damage induced by IR are universal, including base damage, intra-strand cross-link, single-strand break (SSB) and DSB (11). 1 Gy IR can induce around 100,000 ionizations in the nucleus by around 1000 tracks of low LET radiation or 2 tracks of high LET particles (depending on the LET). For low LET radiation, around 2000 base damages, 850-1000 SSBs, around 150 DNA-protein cross-links and 40 DSBs can be induced per Gy per cell (5). All types of DNA damage can be due to the direct or indirect effect. Base damage includes base loss and base modification. A large proportion of

base damage is formed from the interaction of indirectly produced free radicals from water radiolysis. It is estimated that about 80% of hydroxyl radicals ($\bullet\text{OH}$) react with a base which can cause base damage and the remaining 20% of radicals react with sugar moieties which might generate base loss or SSB (12). Although the number of DSB induced per unit dose is lower than that of the other types of DNA damage, it is thought to be the most lethal lesion as both DNA strands are broken simultaneously within a distance of < 20 base pairs (bp).

IR can create clusters of damage which comprise two or more lesions in a 20 bp region on DNA (13). These lesions can be base damage, cross-links and DSB. They pose a challenge to the cellular DNA repair system and if improperly repaired, will cause new DSB, mispairing or deletions. In consequence, clustered damage is expected to be repair resistant, increasing genomic instability and malignant transformation (14). The complexity of the clustered damage is directly proportional to the LET (5). Monte Carlo calculations reveal that there are around 25 lesions per cluster after high LET radiation exposure and only 10 lesions after low LET (15). Clustered damage can be divided into DSB-related and non-DSB oxidative clustered DNA lesions. About 70% of DSB are clustered after exposure to high LET radiation while the number is only 30% when induced by low LET radiation (16). The reason is that the energy deposition by high LET radiation is densely distributed along particle tracks while low LET is widely spread, which influences the probability of clustering. The yield of oxidative clustered damage decreases with increasing LET as was shown both in Monte Carlo simulations and in biological studies with plasmid DNA, linear lambda DNA and Chinese hamster cells (15, 17). It suggests that the biological effect of ionizing radiation which increases with LET is not only related to the yield of clustered DNA damage, but also highly influenced by the complexity of the damage.

DNA damage response

Damage to the DNA is ongoing every second with some 30 000 lesions per day by endogenous factors (18) like byproducts of normal cell metabolism or DNA replication, and can also be induced by external factors like radiation and genotoxic chemicals (19). Maintaining the genome integrity is crucial for survival and the next generation of cells and organisms. Eukaryotes have evolved a complex signal transduction pathway to handle the fate of a cell and

DNA lesions, called DNA damage response (DDR). DDR has the ability to sense DNA damage, transduce this signal and promote the following cellular response to the lesions including appropriate DNA repair, cell cycle regulation, apoptosis and senescence, therefore being an important process in genetic disease, aging, cancer and development. DDR is a complex system including sensors, transducers and effectors, which interplay between protein phosphorylation and the ubiquitin pathway (19, 20).

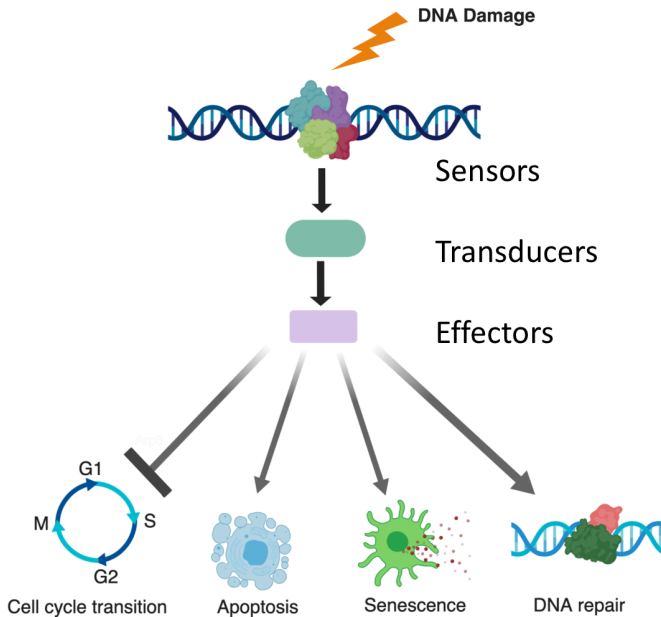


Figure 2. Structure of DNA damage response. Modified from (21)

Repair pathways after DNA damage

Efficient and faithful DNA repair systems can handle DNA damage from endogenous and exogenous damage as well as IR to keep the integrity of DNA. Generally, simple SSB and base damage can be rapidly repaired by base excision repair/single-strand break repair (BER/SSBR) pathways (22). Bulky DNA lesions formed by UV light can be removed by nucleotide excision repair (NER) which is mainly used by mammals (23). Among all the types of

damage, DSB is the most lethal form and one unrepaired DSB can trigger apoptosis. Efficient DSB repair is important for cell survival and function after exposure to IR. There are two main DSB repair pathways in mammalian cells: non-homologous end joining (NHEJ) and homologous recombination (HR) pathways, which will be the target of more focus below (24). NHEJ is a fast pathway to rejoin compatible DNA ends after adding new nucleotides or removing excess ones. It is relatively error-prone, available at any time in the cell cycle, but prevalent in the G1 phase. HR is a slower pathway and uses the homologous DNA strand to restore missing nucleotides. It is error-free and mainly active in the G2 and late S-phase, when sister chromatids have formed and are in close proximity (25). NHEJ is dominant in DSB repair in vertebrates (26). How a cell chooses to activate NHEJ or HR during S/G2 is not well understood. Here, the interaction of tumor suppressor p53-binding protein 1 (53BP1) and breast cancer type 1 susceptibility protein (BRCA1) seems to play a role. BRCA1 initiates HR by activating DNA end resection, while phosphorylated 53BP1 blocks the resection. BRCA1 can push a cell to select HR by promoting protein phosphatase 4C (PP4C)-dependent 53BP1 dephosphorylation and the release of radiation-induced foci (RIF) (27).

In the NHEJ pathway, the protein heterodimer p70/p80 kDa subunit of Ku antigen or XRCC6/5 (Ku70/Ku80) binds to the two free ends generated by DSB within seconds after a break has formed, based on the abundance of Ku and its strong equilibrium dissociation constant for duplex DNA ends (28). Ku:DNA complexes serves as a node or a scaffold, where many proteins can dock. Then the complex can recruit the nuclease (DNA-dependent protein kinase catalytic subunit (DNA-PKcs) and Artemis), polymerase (pol mu and pol lambda) and ligase (XRCC4-like factor (XLF), X-ray repair cross-complementing protein 4 (XRCC4) and DNA ligase IV) in any order (25, 28). This flexibility allows NHEJ to handle identical starting ends and get a diverse array of outcomes. DNA-PKcs binding to the complex and trans-autophosphorylation is an essential step for efficient progression of the NHEJ pathway (29). Non-compatible ends can be modified by removing excess nucleotides by nucleases (Artemis and DNA-PKcs complex) or adding new ones by polymerases (pol mu or pol lambda). Then the two DNA ends can be ligated together by the XLF:XRCC4:DNA ligase IV complex which can ligate not only compatible DNA ends but also non-compatible ones (25).

HR is initiated with the resection of the DNA end to generate a 3' single-stranded DNA region by removing another DNA strand in the 5' to 3' direction (30). Replication protein A (RPA) coats the single-stranded region and will subsequently be replaced by Radiation sensitive 51 (RAD51). RAD51 forms nucleoprotein filaments and promotes invasion of the homologous template strand. DNA synthesis templated by the intact duplex takes place with dissociation of RAD51. Depending on the process, a Holliday junction may be generated, leading to crossover and non-crossover products (11, 31).

There is also another type of DSB repair pathway, which is called microhomology-mediated end-joining or alternative NHEJ (MMEJ/alt-NHEJ) (32, 33). It is initiated by end resection to generate single stranded overhangs with 5-25 bp microhomologous sequences, which help in aligning broken ends, facilitating annealing. This repair is Ku-independent and always results in sequence deletions (33).

Proteins involved in DDR

Ataxia-telangiectasia mutated (ATM) protein kinase regulates the cellular response to DSB in every cell phase by phosphorylating numerous proteins in the DDR network leading to DSB repair, cell cycle arrest or apoptosis (34). ATM is a 350 kDa serine/threonine protein kinase that can be recruited and activated by DSB and other factors like oxidative stress (35). Inactive ATM exists as a dimer or multimer in the cell nucleus, and IR induces rapid ATM autophosphorylation (at Ser 1981 in humans) in its FRAP-ATM-TRRAP (FAT) domain that causes dissociation of ATM homodimer (36). ATM is recruited by the Mre11-RAD50-Nbs1 complex (MRN) at the broken end which is thought to be a platform for ATM and can initiate ATM activation (37-39). Activated ATM can phosphorylate around 200 downstream proteins involved in DNA repair, cell cycle checkpoint control and apoptotic responses, including H2AX, Checkpoint kinase 2 (Chk2), p53, mouse double minute 2 homolog (MDM2), MER2, RAD9, RAD50, DNA-PKcs, Nbs1 and Artemis (40). ATM mediate a two-step cell cycle regulation response to DSB. In the rapid response activated ATM phosphorylates Chk2, which phosphorylates cell division cycle 25A (CDC25A). Phosphorylated CDC25A becomes ubiquitinated and degraded, which leads to phosphorylated Cyclin-dependent kinase 2-Cyclin (CDK2-Cyclin) accumulation and a cell cycle block. In the delayed

response, ATM phosphorylates MDM2 and p53, which also can be phosphorylated by Chk2, resulting in activation and stabilization of p53, leading to an increased expression of Cdk inhibitor p21 (CDKN1A) to maintain long-term cell cycle arrest or induce apoptosis and senescence (41).

Unlike ATM, DNA-PKcs primarily regulates a smaller group of proteins involved in DSB end joining. It is a 470 kDa protein kinase which is activated by binding to Ku70/80. It mainly plays a role in NHEJ as described above as well as in telomere capping and V(D)J recombination (42, 43). DNA-PK also can phosphorylate H2AX at serine-139 (γ H2AX) on chromatin flanking DSB sites to initiate ubiquitin-adduct formation and recruitment of DDR factors to amplify DSB signaling and promote DSB repair (44).

p53 is a well-studied tumor suppressor which plays an important role in the DDR pathway by orchestrating a variety of DDR mechanisms, including DNA repair, transient cell cycle arrest, apoptosis and senescence (45). It is mutationally inactivated in about 50% of human cancers (46). It acts as a transcription factor existing in the nucleus with a size of 53 kDa (47). After exposure to IR, the concentration of p53 increases rapidly. It is regulated by ATM and Chk2 in response to DSB as described, before leading to cell cycle arrest by transcriptionally regulating p21 to allow either repair and survival of cells or apoptosis by transcriptionally regulating proapoptotic bcl-2-associated X protein (BAX) and PUMA/BBC proteins (47). p53 can directly promote NER pathway by regulating NER factors Xeroderma pigmentosum, complementation group C (XPC) and DNA damage-binding protein 2 (DDB2) and induce dNTP synthesis (48). The expression level and activation level of p53 act in an oscillatory mode over the time with ATM pulses which can be detected in single cells (49).

Radiation-related genes

Numerous studies published in recent years suggest that dose- and time-dependent gene expression alterations induced by radiation can be used as a biosimetric markers, especially in peripheral blood lymphocytes (PBL) (50-52). Gene expression changes were usually checked in blood cells or human cell lines 2 to 48 h after exposure to a vast array of doses from tens of mGy to tens of Gy of low LET or high LET radiation by qPCR or microarray (50, 53-

56). A number of radiation-responsive genes, mainly involved in the p53-signaling pathway, have been identified and validated (57). After literature searches on gene expression alterations in these publications, 6 genes were selected and used in our studies to investigate the radiation response: BCL2 binding component 3 (BBC3), CDKN1A, ferredoxin reductase (FDXR), growth arrest and DNA damage inducible alpha (GADD45a), MDM2 proto-oncogene (MDM2) and Xeroderma pigmentosum, complementation group C (XPC). All of them are p53-regulated genes and have a positive response to increased doses of radiation. BBC3 and FDXR are involved in apoptosis. CDKN1A and GADD45a play a role in cell cycle regulation. MDM2 is an inhibitor of p53. XPC encodes a protein involved in NER. GADD45a also has a function in DNA damage repair.

Factors which modulate the biological effects of radiation

Mixed beam effect

As described above, low LET and high LET IR can induce qualitatively and quantitatively different cellular responses. Under many situations, people are exposed to mixed radiation fields of high LET and low LET IR. For example, high natural background IR in the environment from the bedrock is a mixed field of gamma rays (e.g. from ^{226}Ra) and alpha particles (e.g. radon gas) (58). Occupational groups such as flight staff and astronauts receive a mixed exposure to gamma rays, neutrons, protons and cosmic rays (59). Patients during radiotherapy may be exposed to a mixed radiation such as in high energy photon therapy (gamma-neutron reaction) (60) or boron neutron capture therapy (61).

To predict the risk of mixed beams is important for radiation protection and radiotherapy. But whether the combined exposure to high LET and low LET radiation acts in an additive (no interaction) or synergistic (a positive interaction) mode is still not clear. The mixed beam studies were well summarized by Elina Staaf (62). Studies on the mixed beam effect did not yield clear results as some of the results suggested synergism while others additivity. The reason is unclear, but one factor could be that the settings of experiments are too variable to be compared, such as different cell systems, endpoints, sequence of exposure (simultaneous or sequential), radiation qualities (dose and

dose regimes), types of IR and methods of analysis. A mixed beam facility has been set up in our lab which allows simultaneously exposing cells to X-rays and alpha particles. Study results show a synergistic biological response after exposure to mixed beams which is higher than the simple sum of responses induced by single exposure. The kinetics of DNA repair also showed a delay following mixed beam exposure (63-65). The possible explanation of synergism is that: two radiations interact and change the distribution of ionization and excitation; higher chromatin structures may be opened by high LET radiation and DNA is exposed to free radicals induced mainly by low LET radiation; more highly clustered DNA damage is formed which is difficult to repair. Further studies about the mixed beam effect are needed.

Temperature effect at radiation exposure

Many factors can modulate biological effects of radiation, one of which is temperature during exposure. An incubation in melting ice is a common step in most molecular biology labs in order to inhibit or reduce DNA repair, protein synthesis or other cellular response during the experiment process or transportation of samples. Historically, low temperature of cells at exposure was not thought to influence the level of DNA damage, although an increased level of chromosomal aberrations was found (66, 67). Later, more radiobiological experiments have been done which were designed to analyze DNA damage and repair in mammalian cells exposed at the temperature of physiological growth, on melting ice or at room temperature (RT), depending on the experimental conditions. The results indicate that temperature at exposure can indeed influence cellular responses and experimental reproducibility.

In recent years, many studies show that hypothermia (low temperature at exposure) can act in a radio-protective manner which was observed with various endpoints. This phenomenon was termed the temperature effect (TE). Hypothermia during irradiation influences the radio-response of MCF-7 cells because low temperature (2 °C) X-irradiation of these cells (2, 3 and 4 Gy) resulted in higher surviving fractions compared to irradiation at 37 °C (68). Low temperature can reduce the level of chromosome aberrations, especially dicentric chromosomes, after in vitro irradiation of human PBL (69-71). Kempner et al. found that some enzymes had an enhanced enzymatic activity after the same dose of radiation at low temperature compared to RT (72). Both

PBL and thymidine kinase heterozygote cell line (TK6) cells showed lower frequencies of micronuclei (MN) after exposure at low temperature than after exposure at 37 °C (73-75). For human diploid fibroblast cells, rewinding of supercoils was inhibited after irradiation using the fluorescent halo assay and this inhibition of rewinding was reduced when cells were irradiated at low temperature compared with cells irradiated at 37 °C (76). Interestingly, the radio-protective effect of hypothermia is not always seen using different endpoints in the same cell systems. For example, in PBL the TE was seen at the level of MN, but not at the level of DNA damage measured by the alkaline and neutral comet assay (73).

Although the TE was observed and described in many studies, its underlying mechanisms are not so clear. Indirect IR seems to play an important role in hypothermia as a higher TE has been observed after low LET than high LET radiation (77). One study also showed that low temperature could decrease the indirect effect of irradiation though reducing the DNA damage induced by ROS (73). TE had no relationship with the level of γ H2A foci, which means that temperature has no influence on the level of radiation-induced DNA DSB and their repair (71, 75). The ATM kinase-mediated DNA damage signaling is not involved in the TE, but the TE was abolished when the chromatin was forced into a more open conformation through the inhibition of histone deacetylase by trichostatin A (TSA) (75). Selective elimination of highly damaged cells by apoptosis may also explain the TE, but the mechanism remains unknown (78).

From the outcome of the studies above, it indicates that the TE reduces the transformation of DNA damage to chromosomal damage, but no change to the initial DNA damage. The aim of the project was to analyze the kinetics of aberration during the first hours after exposure by premature chromosome condensation (PCC) in order to unravel the mechanism behind TE.

Dose rate

To estimate any biological effect of IR, the absorbed dose and the radiation quality should be known. Beside these, the dose rate, which is the dose delivered per unit time, is also a key factor in determining the effect of a certain dose. Extensive studies suggest that a high total radiation dose delivered at a low dose rate has less biological impact than when it is given at

a high dose rate, the so called dose rate effect. It was also found that a radiation dose given in a series of fractions decreases the biological effect in normal tissue around the tumor. The reason is that radiation delivered at lower dose rate or in series of fractions gives cells time to recover (79). Usually, a range of dose rate from about 0.1 Gy/h (in distant tissues) to several Gy/min is important in radiotherapy. In this range, the fraction of dead cells decreases as the dose rate is reduced when cells are exposed to a given dose, principally because of the repair of sub-lethal damage. In certain cases, an inverse dose rate effect is observed over a narrow range of dose rate in some cell lines and this might be due to cell cycle G2 arrest, which is a radiosensitive phase of the cell cycle (80). This hyper-radiosensitivity occurs in a lower dose rate range of 0.1-1 Gy/min/h (81). Ultrahigh dose-rate radiation given in a short pulse is called FLASH radiotherapy. Recent studies in animals showed that it can maintain tumor control level, while inducing less damage to normal tissue compared to the conventional radiotherapy at a dose rate of ca 1 Gy/min, suggesting that ultra-high dose rate may enhance the therapeutic window in radiotherapy and have a potential clinical applications (82-84).

According to the United Nations Scientific Committee on the Effects of Atomic Radiation (UNSCEAR) (www.unscear.org), a low dose is classified as 0.1 Gy or lower and a low dose rate (LDR) is classified as 0.1 mGy/min averaged over 1h or lower. Any dose or dose rate above these values is regarded as high. In cell or animal experiments, a value of ca 1 Gy/min is generally used as representative for high dose rate (HDR) when comparing the effectiveness of low and high dose rate. This value is mainly based on the most common output of available radiation facilities and also on the fact that this dose rate is used in external beam radiotherapy (84, 85). The International Atomic Energy Agency recommends the dose rate of 1 Gy/min for generating calibration curves to be used in retrospective biological dosimetry for estimating doses received as consequence of accidental radiation exposures (86).

Many experimental studies are carried out to compare the biological effectiveness of HDR with that of LDR. The rationale for this is the prevailing uncertainty regarding the use of the Dose Rate Effectiveness Factor (DREF). Its use was suggested by the International Committee on Radiological Protection (ICRP) when risk factors derived from the Life Span Study (LSS) on Hiroshima and Nagasaki survivors are applied to predict health effects resulting from chronic exposure to radiation (87). However, the atomic bomb survivors were exposed

to tens of Gy/min (88). The important question is whether gamma radiation delivered very high dose rate (VHDR - several Gy/min) is more effective in inducing DNA damage than that delivered at HDR.

Aims

IR-induced biological effectiveness can be influenced by many factors, like the type of cells radiated, the characteristics of the radiation (high LET or low LET radiation), dose rate, temperature and so on. Some of the factors have more clear effects than others. In this thesis, we focused on three factors influencing radiation-induced biological effectiveness: mixed beams of high and low LET IR, low temperature and high dose rate. The specific aims were:

1. To investigate the effect of combined action of alpha particles and X-rays on inducing initial DNA damage and on kinetics of DNA repair by alkaline comet assay in human PBL and DSB repair foci frequency in fixed U2OS cells. DDR was studied at the level of gene expression and protein activation, aiming to uncover the mechanism of the mixed beam effect. The mRNA levels of radiation-related genes were also tested under inhibition of ATM or DNA-PK, after exposure to mixed beams.
2. To study whether low temperature at exposure has a radioprotective effect at the level of cytogenetic damage and if it is due to a reduced effective transformation of DNA damage into chromosomal aberration or not using premature chromosome condensation in isolated lymphocytes. DDR was analyzed by measuring ATM, DNA-PK and p53 phosphorylated levels and mRNA levels of the radiation-responsive genes.
3. To test the biological effectiveness of very high dose rate (8.25 Gy/min) compared to high dose rate (0.79 Gy/min and 0.39 Gy/min) by different endpoints, aiming at investigating the validity of the dose and dose rate effectiveness factor at ca 1 Gy/min.

Materials and Methods

U2OS cell line and 53BP1 foci

The human osteosarcoma U2OS cell line, which was isolated from a moderately differentiated sarcoma of the tibia of a 15-year-old girl in 1964, is one of the first generated cell lines and widely used in biomedical research (89). Conventional cytogenetic analysis and spectral karyotyping have showed the character of chromosomal instability, including high incidence of aneuploid and a large number of chromosomal aberrations (90). The tumor suppressive gene p53 was found functional in U2OS cells and can regulate p53-dependent cell cycle arrest and apoptosis induced by DNA damage (91, 92). U2OS cells were cultured in Dulbecco Modified Eagles Medium, supplemented with 10% bovine calf serum and 1% penicillin streptomycin, in 5% CO₂ humidified air at 37°C.

U2OS cells stably expressing green fluorescent protein (GFP) tagged protein 53BP1 at its NH₂ terminus were kindly provided by C. Lucas from the Danish Cancer Society, Copenhagen, and the cells were characterized and applied in this article (93), showing the function of 53BP1-GFP dynamic assembly at the sites of DNA DSB areas to form foci. In our study, cells were fixed with formaldehyde after irradiation and incubation, then pictures were taken under a fluorescent microscope with a 100X oil immersion lens, a Cool Cube 1 CCD camera and the image analysis system ISIS. A modified macro, written for the ImageJ software was used to calculate the area and number of 53BP1 in **Paper I**.

Blood

Fresh peripheral blood was donated by healthy male non-smokers. Ethical permission was obtained from the local ethical committee at the Karolinska University Hospital, Stockholm, Sweden. Whole blood was used in the comet assay and gene expression analysis in **Paper III** and **V**. Isolated human PBL by

Ficoll-Paque premium solution were employed in the western blot and gene expression analysis in **Paper II** and **IV**.

Irradiation

A mixed-beam facility in the Center for Radiation Protection Research at the Department of Molecular Biosciences, the Wenner-Gren Institute, Stockholm University was used for the mixed beam experiments. It consists of an alpha irradiator AIF 08 (241Am, 50 ± 7.5 MBq) on the top and an YXLON SMART 200 X-ray tube (operating at 190 kV, 4.0 mA, no filtering) underneath, which allows exposure to alpha particles and X-rays simultaneously, as described in details by Staaf et al (94). A movable shelf was used to position the polyamide (PA) disc with cells at a defined distance from the alpha source, to control the exposure (on/off). The dose-rate of alpha radiation was 0.223 Gy/min by calculation at the entrance to the cell suspension and the average LET was 90.92 ± 8.55 keV μm^{-1} . The alpha source also emits beta and gamma rays with a maximum energy of 70 keV and a dose rate of 25 mGy/min, which was ignored in the study. The dose rate of X-ray was 0.068 Gy/min in the bottom and 0.052 Gy/min in the top position of the movable shelf because of the different distances to the X-ray tube. The exposure to mixed beams always started in the top position with alpha particles and X-rays acting simultaneously. Then, after reaching the desired alpha dose, the shelf was moved to the bottom position with X-rays on. X-rays was switched off after reaching the desired X-ray dose. In total, the mixed beams dose was always composed of 50% alpha particles and 50% X-rays.

The PA disc have a round, flat well with a depth of 30 μm and 145 mm in diameter. For attached cells, coverslips with cells were put on the top of the disc, a small volume of medium was added and the disc was covered with a 2.5 μm Mylar foil lid. For cell suspensions or blood, 250 μl was added on the disc, covered with the lid and smeared out evenly. The Mylar foil and the thin layer of medium allow alpha particles to pass through and reach the cells. No collimator was used during the cell exposure because a significant reduction to the alpha particle dose rate would results from the long source-cell layer distance.

Gamma radiation from three ^{137}Cs sources at the Stockholm University was used in the TE and dose rate experiments: 1) Scanditronix (Uppsala, Sweden)

delivering a dose rate of 0.39 Gy/min; 2) Gammacell 40 Exactor (AECL, Canada) delivering a dose rate of 0.79 Gy/min and 3) Gammacell 1000 (AECL, Canada) delivering a dose rate of 8.25 Gy/min.

Western blot

Western blotting is an important and common biochemical technique used in identifying specific proteins from a complex mixture of proteins extracted from tissues or cells. It contains three main steps: (1) Denatured proteins are separated through gel electrophoresis based on their molecular weights. (2) Separated proteins are transferred onto a membrane. (3) A proper primary and secondary antibody are used to visualize the target protein (95). Western blot was used in **Paper I, II IV** to assess the phosphorylation level changes of DDR proteins (p-DNA-PKcs, p-ATM, p-p53) before and after IR. Glyceraldehyde-3-phosphate dehydrogenase (GAPDH), a key enzyme of glycolysis, was used as housekeeping gene since its expression is minimally responsive to IR (96).

Comet assay

Comet assay or single-cell gel electrophoresis is a common and widely used technique to quantify and analyze DNA damage and DNA repair in individual cells. Simply, treated cells are embedded in low melting point agarose on a slide and lysed to release the DNA. Then, negative charged DNA fragments are forced to move to the anode side by electrophoresis to form a comet structure with a brightly fluorescent head (the undamaged DNA part) and a tail (fragmented DNA), observed by fluorescence microscopy. The percentage of DNA in the tail shows a proportional relationship to the frequency of DNA breaks, which can be analyzed by special comet assay software linked to the microscope (97, 98). The comet assay measures transient DNA damage because of the short time between the treatment and the detection. DNA repair kinetics can be measured by incubating cells after treatment which analyses DNA damage in different time intervals (98). The comet assay can be used not only in vitro like for immortalized cell lines, but also in vivo for any tissue that can be separated to single cell suspensions, in the fields of genotoxicity testing, ecotoxicology, human biomonitoring, molecular epidemiology and fundamental research in DNA damage and repair.

Comet assay has many variants which can detect different DNA lesions. Neutral comet assay with a neutral condition during unwinding and electrophoresis only can detect DSB (99). Under alkaline conditions, a very high pH solution (>13) can unwind the double stranded DNA to single stranded. So SSB can increase the DNA fragment migration through the gel as well as DSB. The alkaline comet assay can assess both DSB and SSB, and also alkali-labile sites which can be converted to SSB in the alkaline conditions (100, 101). The alkaline comet assay was applied in **Paper II** to assess the initial DNA damage and the DNA repair kinetics after radiation with lymphocytes in peripheral whole blood.

Other lesions, such as oxidative DNA damage can be detected using special DNA repair enzymes which can convert them into SSB in the comet assay. Formamidopyrimidine [fapy]-DNA glycosylase (Fpg) is a glycosylase in *E. coli* which can cleave specific DNA lesions. The majority of substrates are oxidized purines like FapyGua, FapyAde, C8-oxoAdenine, and to a lesser extent, other modified purines and some abasic sites. Endonuclease III (Endo III) can cleave specific DNA lesions and the majority of substrates are oxidized pyrimidines like thymine residues damaged by ring saturation, fragmentation, or ring contraction including thymine glycol and uracil residues, FapyAde, 5-OH-Cyt and to a lesser extent FapyGua, some abasic sites. Oxidative clustered DNA lesions, which are located within 10-20 bp, can be induced by low dose ionizing radiation, are very difficult to repair and produce cytotoxic and mutagenic effects. Bi-stranded oxidative clustered DNA lesions can form DSB after treatment with Fpg or Endo III and the DSB can be detected by neutral comet assay (102, 103). This kind of comet assay, called enzyme modified comet assay was attempted in the study of mixed beams but did not succeed.

The cytokinesis-block micronucleus assay

The cytokinesis-block micronucleus (CBMN) assay is a method to visually determine DNA damage at the chromosomal level in single cells. It is widely used in detection of IR-induced chromosomal aberrations since it can measure both chromosome loss and chromosome breakage. MN originate from either lagging chromosomes or acentric chromosome fragments at anaphase and they are easily identified, as they are morphologically similar to, only smaller, than the main nuclei. As MN cannot be seen in non-dividing cells, Cytochalasin-B (Cyt-B) is used to stop cytokinesis when cells undergo mitosis,

thus allowing the formation of binucleated cells (BNC), or tri- and multinucleated cells, depending on Cyt-B culturing time and dose. MN are only scored in BNC to ensure that the scoring is restricted to cells that have divided only once after irradiation. Scoring the number of nuclei per cell gives the replication index, which indicates the rate of cell division. The CBMN assay can only be applied in cells that will divide after exposure and phytohemagglutinin is needed to stimulate cell proliferation in study of lymphocytes (104, 105).

Quantitative PCR

Quantitative polymerase chain reaction (qPCR), also called real-time PCR, is an efficient and rapid method for nucleic acid detection based on the traditional PCR with improvements in detection and quantification of small amounts of starting material by using a variety of fluorescent dyes that can correlate PCR product amount to fluorescence intensity (106). In our experiment, mRNA was reversed transcribed to cDNA before qPCR, but it can also be performed before qPCR in a single tube. The cycle threshold (Ct) is recorded when the fluorescence intensity of a target is first detected during amplification. The more target cDNA in the starting material, the quicker a fluorescent signal will appear, yielding a lower Ct (107). Both absolute quantitation and relative quantitation can be quantified. The comparative C_t ($2^{-\Delta\Delta C_t}$) method was used in the projects for calculating changes in gene expression as a relative fold difference before and after exposure.

18S rRNA was used as a housekeeping gene because rRNAs are transcribed with a different polymerase and rRNA expression tends to be less affected by treatments than mRNA (108). 18S may keep intact in samples with degraded mRNA while 28S may not (109).

Premature chromosome condensation

Usually eukaryotic chromosomes condense during mitosis, which is strictly regulated by the cell cycle machinery. But under many situations, chromosomes can condense outside of mitosis. This is called premature chromosome condensation (PCC) and the condensed chromosomes are called prematurely condensed chromosomes (PCCs). The PCC phenomenon was first reported in virus-infected mammalian cells about half a century ago (110, 111). Then, PCC was found in cells fused with mitotic cells using fusogenic virus or chemicals such as polyethylene glycol. Fusion-PCC using polyethylene glycol is

established in the cytogenetic field which depend on the production of substantial amounts of mitotic-arrested inducer cells (112, 113). This method was applied in **Paper V**. Today, drug-induced PCC is possible by applying phosphatase inhibitors like okadaic acid or calyculin A and is used in diverse research areas, such as radiation biology for chromosome analysis since this method is much simpler and easier than fusion-PCC (114, 115).

Envelope of additivity analysis

The envelopes of additivity model was applied to analyze the effect of interaction between alpha particles and X-rays in inducing DNA damage and DDR gene expression. It relies on the dose response curves in described in **Paper I, II and III** (116) and is used to test the significance of an interaction when at least one of the dose response curves is not linear. Two isobolograms are constructed which are based on assuming heteroadditivity or isoadditivity of the effect induced by a combined exposure. Heteroaddition is the result for independently acting agents, while isoaddition is the result for mechanistically similar agents. In the heteroadditivity mode, the effects of dose D_A and D_B are added to result in effect E_C . In the isoadditivity mode, the effect to be added to E_A from agent B corresponds to that if the system had been treated with a dose of agent B up to an effect equivalent to E_A . The remaining dose D_B needed to attain the combined effect E_C is smaller than in the case of heteroaddition. If an observed effect is inside the envelope, it indicates additivity. If an effect lies below the envelope, it indicates a synergistic effect. A location above the envelope indicates a sub-additive effect (117). Usually, 3 different levels of effect are tested for interaction by envelopes of additivity.

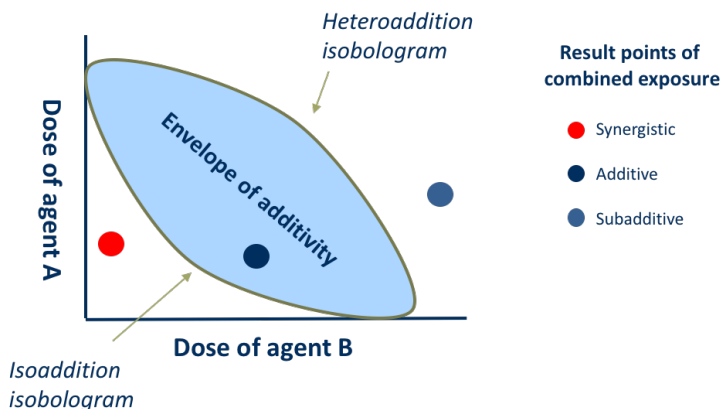


Figure 3. Constructing two isobolograms based on assuming the two forms of interaction.

Results and Discussion

Paper I

To investigate the possible interaction of combined IR, a mixed-beam exposure facility was constructed in our lab, which can be used to expose cells to X-rays and alpha particles simultaneously (94). Previous studies showed a synergistic effect of mixed beams in inducing micronuclei and complex aberrations in PBL (63, 65). But the mechanism is unclear. In **Paper I**, U2OS cells, which are stably expressing DNA repair protein 53BP1 fused with GFP, were used to verify whether a combined exposure leads to an altered DNA damage response that is different from simple additivity of single mixed-beam components. 53BP1 is a DSB sensor and can form foci at the site of DSB at the early stage of the repair process. The induction and repair of DNA DSB damage, which is visible as formation and disappearance of 53BP1 foci were investigated after exposure to X-rays, alpha particles and a 1:1 combination of both. The dose response relationship of foci induction measured 30 min after exposure between 0 and 2 Gy and the kinetics of focus decay between 0 min to 24 h after exposure to a dose of 1 Gy were detected. The phosphorylated levels of DSB response markers, ATM and p53, were quantified too.

Particle radiation can deliver high energy in small subcellular volumes which lead to clustered DNA damage, including DSBs (118). Low-LET-induced foci tend to be fast repaired, while high-LET radiation will lead to clustered DSBs, the repair of which is delayed and largely relies on homologous recombination (119). The larger size of foci indicates complex DNA DSBs on chromatin (120-122). According to the distribution of focus areas, foci were divided into small foci (SF) and large foci (LF) with the threshold of $0.5 \mu\text{m}^2$ (40 pixels). Construction of envelopes of additivity was used to test synergistic or additive effects of the interaction of X-rays and alpha particles according to the dose response curve of foci per cell. The result showed that mixed beams induce DNA damage in a synergistic way for both SF and LF at all three tested focus level. The 53BP1 focus repair kinetics showed that the radiation quality

strongly influenced the focus frequency decay. The decline-speed was lowest after mixed beams exposure at the quick repair period (the first few hours after exposure). This mixed beam-induced synergistic effect of DNA DSB repair was not only visible at the level of all foci and SF, but particularly obvious in the decay of LF. ATM and p53 was activated by all radiation types as detected 1 h, 3 h and 6 h postirradiation, with the weakest induction observed after 1 Gy X-ray irradiation. The X-ray-induced level of p-ATM and p-p53 declined during the investigated 6 h time frame but not that of alpha particles or mixed beams, indicating the maintenance of damage signaling by persistent high LET-induced damage.

There are two possible ways of mixed beams interaction. Our results do not support the hypothesis, that mixed beams can increase the energy deposition, LET, and consequently of DNA damage complexity. No evidence of increased focus area due to mixed beams could be detected.

Another mechanism of interaction between low and high LET radiation could be that exposure to either low or high LET radiation engage the DNA damage response machinery to the extent that the other damage induced by the high or low LET radiation may not be repaired properly in time. Indeed, the analysis of the kinetics of focus decay revealed that the initial elimination of foci induced by mixed beams proceeded more slowly than expected, which is largely linked to LF. Moreover, the higher level of activated ATM and p53 after exposure to mixed beams and alpha particles compared to X-rays, which was kept for a prolonged time, also may be interpreted as evidence of an overwhelmed DNA repair system.

We found that alpha particles induced a higher percentage of LF than X-rays and mixed beams at 0.5 Gy and 1 Gy, which fitted to our expectation that high LET IR induces more complex damage. But mixed beams induced LF had no increase in their proportion relative to X-rays. The proportion of large foci did not increase with increasing radiation dose for all radiation types, demonstrating that it is related to radiation quality and not the level of DNA damage. Here, it must be recalled that a synergistic effect of mixed beams was observed for both large and small foci and that the combined action of both radiation types does not result in an increased LET. Rather, there is more simple damage induced after mixed beams exposure.

A more successful repair outcome in mixed beam-exposed cells relative to alpha particle-exposed cells at 24 h postirradiation, indicate that, after early repair retardation, mixed-beam radiation may be able to increase the slow repair at sites of clustered DNA damage. This phenomenon might be related to the fact that only half of the alpha dose contributed to the effect in mixed-beam-irradiated cells. Further research is required to highlight this point in more detail.

In conclusion, the results suggest that X-rays and alpha particles interact, leading to a synergistic effect, which was higher than accurately predicted based on assuming simple additivity of the individual mixed-beam components. It is not only present at the level of induction of DNA damage but also at the level of delay of repair kinetics. Our data strongly suggest an overpowering of the DNA repair system in cells exposed to mixed beams, leading to a slow repair of simple and complex damage.

Major finding in **Paper I**

- X-rays and alpha particles interact in producing DNA damage at the level of all tested focus frequencies.
- The decay of mixed beam-induced 53BP1 foci at a slower rate than expected based on simple additivity between the action of X-rays and alpha particles indicates an overpowering of the DNA repair system in cells exposed to mixed beams.
- The slow repair kinetics was mainly due to a reduced initial decay of LF.

Paper II

Unlike cancer cells which were used in **Paper I** to investigate the mixed beams interaction, normal cells (PBL) were tested in **Paper II** and **III**. In **Paper II**, alkaline comet assay was applied to check the level of the initial damage and the kinetics of DNA repair after combined exposure to X-rays and alpha particles or each single exposure respectively from 0 to 2 Gy. Alkaline comet assay can detect not only DSB but also SSB and alkali-labile sites. Relative tail intensity (RTI), which means the percentage of DNA in comet tail, was used as measure of the level of DNA damage. Activation of DDR proteins, DNA-PKcs, ATM, and p53 were detected by western blot in phosphorylated form 1 h and 3 h postirradiation of 2 Gy. The mRNA expression levels of DDR related genes, BBC3, CDKN1A, FDXR, GADD45a, MDM2 and XPC, were investigated in PBL by qPCR after 4 h, 24 h and 48 h incubation following 2 Gy exposure with X-rays, alpha particles and mixed beams.

Dose response curves of RTI showed that mixed beams and X-rays induced higher DNA damage than alpha particles, which were significant at 1.5 Gy and 2 Gy, while the curves of mixed beams and X-rays almost overlapped by each other. The dose response relationship tended to be saturated with increasing dose for all radiation types. The analysis of envelopes of additivity showed that the mixed beams always induced a higher than expected level of RTI at three different damage levels, indicating a synergism of X-rays and alpha particles in inducing DNA damage. The strongest interaction was at the low level of damage, while the weakest was at the highest level of damage.

For DNA repair kinetics, no significant differences were seen in the normalized repair curves among the different exposures, although cells exposed to mixed beams showed a decayed repair compared to X-rays and alpha particles. The delay was also observed in the RTI distributions which demonstrates that the repair of DNA damage induced by mixed beams was less efficient than X-rays or alpha particles.

Irradiation with mixed beams induced the highest activation of ATM and p53 at both 1 h and 3h, which indicated a synergistic effect. A somewhat different result was that DNA-PKcs, after 1h post exposure, was most strongly activated following exposure to alpha particles. However, after 3h post exposure its level turned to be significantly higher for mixed beams than after alpha particles and X-rays.

The levels of 6 radiation-responsive genes' mRNA were lowest 4 h post exposure, highest at 24 h post exposure and intermediate at 48 h post exposure. Although not significant in all cases of analyzed genes, the mRNA levels of all genes were highest in cells exposed to mixed beams, especially at 48 h post exposure.

In summary, the alkaline comet assay result confirmed the previous findings that X-rays and alpha particles interact in inducing initial DNA damage in a synergistic way, which was above the predicted level by assuming additivity of single radiations, and the repair of damage was declined. The results of activation levels of DDR proteins and mRNA expression levels indicated that exposure to mixed beams present a tough challenge for the cellular DDR system.

Major findings in Paper II:

- X-rays and alpha particles interact and produce a synergistic effect in inducing initial DNA damage.
- The repair of DNA damage in cells exposed to mixed beams is delayed.
- The activation level of DDR proteins and the mRNA levels of radiation-related genes were highest in cells exposed to mixed beams.

Paper III

In **Paper II**, the result showed that mixed beams interaction influenced the DDR related gene expression. These selected genes, BBC3, CDKN1A, FDXR, GADD45a, MDM2 and XPC, are involved in the p53-signaling pathway. In **Paper III**, qPCR was used to measure the relative expression levels of the 6 selected genes 24 h following exposure to alpha particles, X-rays and mixed beams (half dose of alpha particles and half dose of X-rays) from 0 Gy to 2 Gy in PBL from 4 donors. The mRNA level of the genes was also tested 24 h following exposure to three different radiation types at 1 Gy under inhibition of ATM or DNA-PK in PBL from 2 donors. The two donors' intrinsic radiosensitivity was compared with the dose response curves for gamma radiation-induced micronuclei.

The dose response curves of 6 genes relative levels in PBL from 4 donors were plotted. All genes showed a positive relationship to exposure. Alpha particles and mixed beams induced similar mRNA expression level increase for most genes and the increased folds were much higher than for X-rays, especially at lower doses. Generally, the dose response curves of alpha particles and mixed beams almost overlapped with each other, while the dose response curve of X-rays was much more linear. A rapid increase in gene expression at lower doses and a saturated increase speed at higher doses were observed after exposure to alpha particles and mixed beams, compared to the more linear increase in gene expression in cells exposed to X-rays. Among all genes, the expression of FDXR was highest, demonstrating that it is the most sensitive marker of IR exposure.

The FDXR gene was chosen to construct the envelopes of additivity analysis at low, medium and high levels of excess levels, according to its gene expression dose response. Mixed beams showed a synergistic effect at all three levels in inducing FDXR expression in Donor 1 and 3, while effects were synergistic at low and medium excess levels, but additive effect at the high excess level in Donor 2. Donor 4 was different from the others. An additive effect was present at a low expression level, but sub-additive effects at medium and high levels were observed. The result suggested that an individual difference may be present for the mixed beam interaction.

To confirm if an individual difference was existing or not, the changes in gene expression induced by 1 Gy X-rays, alpha particles or mixed beams exposure

respectively were analyzed in PBL of Donor 3 and Donor 4 after 24 h incubation in two separate trials (dose response experiment and inhibition experiment). The interval time of the two experiments was about 1 year. The result indicated that the synergistic effect of mixed beams was reproducible in Donor 3, while for Donor 4, the mixed beam effect transferred from an additivity to a synergism. MN assay was used to analyze the intrinsic radio-sensitivity of Donor 3 and Donor 4. The dose response curves of the MN frequency after exposure of gamma radiation from 0 to 2 Gy were plotted. There was no significant difference between Donor 3 and Donor 4 at the MN level. The result suggested that factors other than the individual genotype influence the radiation response of mixed beams.

ATM, but not DNA-PK inhibition, reduced the radiation-related gene expression, but differently for alpha radiation between the two donors. The lower DDR gene expression induction upon inhibition of ATM was significant after exposure to X-rays and mixed beams in Donor 3, while it was significant for all three exposure types in Donor 4. The decrease tended to be larger after exposure to X-rays compared with alpha particles and mixed beams, but it was not significantly different.

In conclusion, synergy in gene expression was present for all donors but the results suggest individual variability in the response to mixed beams, most likely due to life style changes or environmental factors, as no difference in intrinsic radiosensitivity was observed. But this conclusion remains speculative because few individuals were analyzed. The FDXR gene is suggested to be a suitable biodosimeter which has different dose response shapes of low LET and high LET radiation and mixed beams. Alpha particles or mixed beams enhance DDR gene expression much higher at low doses than X-rays and the difference was smaller at high doses as the expression seemed saturated. This explains why the synergetic effect was larger at lower damage levels compared to higher levels.

Major finding in Paper III:

- A synergy of mixed beams was found in DDR-relative gene expression.

- The synergy has individual variability which most likely is due to environmental factors
- The gene FDXR is suggested to be a good biosimulator of radiation exposure, which has different expression patterns between cells exposed to X-rays and alpha particles (or mixed beam), similar to the other genes.
- ATM, but not DNA-PK inhibition, reduced the radiation-related gene expression

Paper IV

Apart from radiation quality and mixed exposure, low temperature at exposure can influence the biological result. Usually, it has a radioprotective manner at the level of cytogenetic damage. The aim of **Paper IV** was to analyze the kinetics of aberration formation during the first hours in order to confirm if the effective transformation of DNA damage to chromosomal damage plays a role during hypothermia (low TE). The technique of PCC was applied in PBL exposed to gamma radiation of 5 Gy at 0.8 °C and 37 °C. In addition, DDR was detected by testing the levels of phosphorylated DDR proteins ATM, DNA-PK and p53 by western blot in PBL 1h following exposure to 2 Gy at 0.8 °C and 37 °C and mRNA levels of radiation-response genes BBC3, CDKN1A, GADD45a, MDM2, FDXR and XPC by qPCR in PBL 24 h following exposure to 2 Gy at two different temperatures.

PCC results showed that the frequency of radiation-induced PCC fragments decreased with time. The frequencies of aberrations per cell in cells exposed at 0.8 °C were significantly lower than in cells at 37 °C, at 0.5 h, 2 h and 4 h post exposure. The same result was observed for excess acentric fragments, dicentric chromosomes and rings scored in mitotic cells at 48 h post exposure. 1 h after exposure, a significantly higher level of activated ATM and DNA-PK was seen, while the level of phosphorylated p53 was significantly reduced. No significant differences were found in each gene expression level in PBL exposed at the two temperatures. After normalizing the mRNA levels in cells exposed at 0.8 °C with the mRNA levels in cells exposed at 37 °C, a significantly lower level of gene expression was observed in cells 4 h after exposed at low temperature compared to high temperature. But at 24 h post exposure, the result was reversed.

The results indicated that the TE is seen as early as 0.5 h, when a reduced frequency of PCC breaks was observed in cells exposed at 0.8 °C compared to 37 °C. And this difference remained until 48 h when cells reach the first mitosis. This result confirmed earlier conclusions (78, 123) that the TE observed at the level of chromosomal aberrations or micronuclei after division is not due to cell cycle modulation or selective elimination of highly damaged cells by apoptosis. The augmented activation of ATM and DNA-PK at 0.8 °C suggested a more effective DDR.

In early studies, no TE was detected at the level of DSB induction and repair by comet assay or gamma H2AX and cell survival or apoptosis (71, 73, 75). It is difficult to explain why the difference in cytogenetic damage level induced by TE is not reflected at the level of DNA damage and cell survival. Maybe the difference of cytogenetic damage is too small to be reflected at the level of cell survival, or the methods we used to study the DNA damage and repair do not measure the fidelity of DNA repair, resulting in the formation of chromosomal aberrations. Either way, more studies are needed here.

Major finding in Paper IV:

- Irradiation of cells at 0.8 °C appears to promote DNA repair to a reduced transformation of DNA damage into chromosomal damage as compared to 37 °C.
- This effect is carried out from the first 30 min post-exposure.
- The TE might be due to an effective DDR with the involvement of ATM and DNA-PK, but not p53.

Paper V

Dose rate is thought to be another factor that can influence the biological outcome, which is important in estimating health effects resulting from the Life Span Study on Hiroshima and Nagasaki survivors to those from chronic exposure to radiation. Usually, a dose rate of around 1 Gy/min is used in cell or animal experiments as representative for HDR. However, the atomic bomb survivors were exposed to tens of Gy/min. The aim of this study was to compare the biological effectiveness induced by gamma radiation delivered at VHDR (8.25 Gy/min) with that induced by HDR (0.38 Gy/min or 0.79 Gy/min).

mRNA levels of FDXR, GADD45a and MDM2 were detected by qPCR at 24 h post irradiation in PBL which were exposed to 0, 1, and 3 Gy of gamma radiation delivered at 0.39, 0.79 and 8.25 Gy/min. Micronuclei and cell proliferation were analyzed in PBL harvested 72 h after exposure. In order to validate the results achieved with PBL, U2OS-53BP1 cells were used to check the frequency and size of 53BP1 foci after 0 min to 24 h following 3 Gy of gamma radiation delivered at 0.39 and 8.25 Gy/min. Clonogenic cell survival was carried out in U2OS cells irradiated at RT with 0, 0.25, 0.5, 0.75, 1, 2, 3, and 5 Gy at dose rate of 0.39 Gy/min or 8.25 Gy/min. Micronucleus assay was also applied in U2OS cells exposure with 0 to 3 Gy at dose rate of 0.39 Gy/min or 8.25 Gy/min. Data were analyzed and dose response curves were plotted.

For PBL, the mRNA levels of FDXR, GADD45a and MDM2 increased with the dose. The highest dose rate 8.25 Gy/min induced the highest effect. The dose response curves of 8.25 Gy/min showed a strong curvature, while the curves of 0.39 and 0.79 Gy/min were closed to linear. MN showed a similar result as 8.25 Gy/min produced the highest MN frequency and the dose response curve was almost linear, which the curves for 0.39 and 0.79 Gy/min had distinct curvatures. Although 8.25 Gy/min caused a highest dose rate effect in these two experiments, the differences compared to lower dose rates were not significant due to high standard deviations.

53BP1 foci assay showed that the level of foci induced by gamma rays delivered at 0.39 Gy/min was higher between 0 to 30 min post exposure and reached the maximal frequency of foci earlier than after 8.25 Gy/min. After that, the frequency of foci induced by 0.39 Gy/min decayed faster than foci induced at 8.25 Gy/min. There was no significant difference in comparing clonogenic cell survival in U2OS cells exposed to gamma rays at 0.39 and

8.25 Gy/min. Consistently higher MN frequencies were observed in U2OS cells irradiated at 8.25 Gy/min compared to 0.39 Gy/min, except cells harvested 30 h post exposure. The shapes of the dose response curves were different too. The curves for 0.39 Gy/min were mainly linear tested in cells harvest 30 h and 48 h postexposure, while the others were saturated at the higher doses.

In summary, the results strongly indicated that gamma rays delivered at VHDR is more effective in inducing DNA damage than that delivered at HDR in both PBL and U2OS cells. In PBL, the dose response curve of gene expression is downward linear-quadratic for alpha particles and linear for photons (Paper III). For MN assay in PBL, linear or saturating dose response relationships are observed for alpha particles (124, 125), while upward linear-quadratic dose response relationships are common for low LET radiation like photons (126). Thus, the dose response relationship of gamma radiation at 8.29 Gy/min is similar with high LET radiation both in gene expression and MN assay, while the dose response relationship of that at 0.39 Gy/min or 0.79 Gy/min is similar with low LET radiation. This indicated that gamma radiation at VHDR induced more complex damage than that at HDR.

The conclusion was confirmed by the results obtained in U2OS cells. The formation and decay of IR-induced repair foci (IRIF) induced by VHDR had a delay and persisted longer than those induced by HDR. MN were also applied in U2OS cells and the MN frequency was higher after VHDR radiation as compared to HDR. The shapes of the dose response curves for MN were different from that in PBL which is related to the fact that U2OS cells were irradiated during asynchronous growth, while PBL were irradiated in the G0 phase of the cell cycle. But VHDR radiation effects in retarded DNA repair kinetics and high level of chromosomal aberrations did not lead to a low level of clonogenic cell survival, as chromosomal damage does not induce complete impairment of the reproductive capacity of cells (126).

Major finding in Paper V:

- Gamma rays delivered at VHDR is more effective in inducing DNA damage than that delivered at HDR in both PBL and U2OS cells

- DSB repair had a delay after exposure to VHDR gamma radiation compared to HDR radiation.
- The shape of dose response curve in PBL exposed to gamma rays at VHDR is similar as high LET radiation, which is different than that at HDR, indicating that VHDR gamma rays can induce more complex damage.
- There is no difference in clonogenic cell survival in U2OS cells when comparing VHDR and HDR.

Conclusions and future studies

Radiation biological effectiveness is influenced by many factors when cells are exposed to the same dose. In the first three papers, the interaction of mixed beams which contains half low LET (X-rays) and half high LET radiation (alpha particles) was studied. The possibility of an interaction of different radiation quality is not considered in calculation of the biological effect of mixed beams for radiological protection. Our results strongly suggested a synergistic effect of mixed beams which is higher than simple additivity. Simultaneous exposure to X-rays and alpha particles not only induces DNA damage synergistically, but also enhances the DDR system much higher than additivity. Moreover, the DNA repair system is overwhelmed by the damage leading to a delay of repair. It was also found that the dose response of gene expression is different between X-rays and alpha particles. In **Paper IV**, low temperature at exposure was investigated. We found one of the mechanisms of TE was through promoting DNA repair to a reduced transformation of DNA damage into chromosomal damage. Moreover, a dose rate effect was detected in **Paper V**. The data showed that gamma rays delivered at VHDR are more effective in inducing DNA damage than when delivered at HDR. The shape of dose response curve in PBL exposed to gamma rays at VHDR is similar to the curve for high LET radiation, while that at HDR is like low LET radiation, indicating that VHDR gamma rays can induce more complex damage. Cells irradiated at different cell cycle phases might influence the dose response curve.

The results are meaningful for the perspective of radiation protection and risk prediction for exposures to a mixed field, at low temperature or at VHDR. Although the levels of health risk cannot be calculated from our results, the data suggest that these factors should be considered when risk factors are transferred between cohorts exposed to different radiation qualities and dose rates.

The mechanism of the synergistic effect of mixed beams was studied, but unfortunately, the enzyme-modified neutral comet assay did not succeed because of the limitation of dose and dose rate of our mixed beams facility. This kind

of comet assay can test bi-stranded oxidative clustered DNA lesions and need a higher dose than we can achieve. We cannot conclude if the complexity of DNA damage induced by mixed beams increased or not. A high resolution analysis of DSB repair foci by transmission electron microscopy (TEM) is undergoing to detect the organization and localization of DSB repair-related proteins. The high magnification and resolution of TEM permits visualization of the intracellular distribution of repair proteins at the single protein level. It is very interesting to use this method in order to visualize foci involved in the recognition and repair of DNA damage in cells exposed to mixed beams of high and low LET radiation. It will be possible to measure, with high resolution, the size of the foci as a function of time after exposure to mixed beams. The results will yield fascinating information about the complexity of the damage (focus size) and the distribution of the foci in the cell nucleus (eu-/heterochromatin). Monte Carlo simulation can be used here to help understand the interaction of mixed beams by theoretically calculating the dose distribution and biological damage in DNA based on experimental data.

The result showed that the gene expression assay is a rapid and convenient method to test radiation dose and quality. It is worth to test the influence of other signal pathways in order to discover mechanisms behind the effect of mixed beams, TE or dose rate. Several biomarker genes were found alternatively transcribed or spliced after irradiation (127) and investigating gene expression at the single exon level should be considered in our future studies.

Acknowledgments

First and foremost I'd like to express my sincere gratitude to my supervisor **Andrzej Wojcik** who accepted me first as a master project student, then as a PhD student. Your guidance is so helpful both in science and in daily life. Your patience and positive attitude encouraged me to overcome most of the challenges during my PhD study. Thank you for organizing the interesting trips and sport. Thank you for all of the support in the past 5 years.

Siamak Haghdoost, my co-supervisor, thanks for all the dedication to my project. Thanks to **Mats Harms-Ringdahl** for the scientific discussions and useful advices.

Big thanks to my co-supervisor, **Lovisa Lundholm** for technical support, scientific guidance and encouragement to go further. Thanks for the help in manuscript and thesis writing.

Halina Lisowska, I am very glad and proud to have collaboration with you and publish articles together. Thanks for all the help during the collaboration.

I am very grateful to previous and current group members who made direct and indirect contribution to my project: **Beata**, for statistic help and wonderful movie nights. **Alice**, for guiding me in the lab from the very beginning and technical help in the lab. I can not forget the tasty tiramisu for the parties. **Pamela**, for every qPCR plate you collected for me in the late evening. **Mila**, for having nice daily talks in and out of science. I enjoyed the time working with you all.

And also thanks to the old or new members of "big" Radbio group: **Ainars**, **Asal**, **Eliana**, **Elina**, **Karl**, **Sara S**, **Sara SM**, **Traimate**, **Ali**, **Gunilla**, **Ayumi**, **Alexandru** and **Paulo**, for all your help in the lab and the time we spent together. Thank you for making a nice working atmosphere and for happy time during all the dinners and parties.

Siamak and **Noushin Emami**, great thanks for the help of blood drawing! And thanks to all my blood donors who I cannot mention the names here. Without you guys, I could not do my projects.

I'd like to thank my intelligent students in the projects and courses. Thanks for the trust and I learned a lot during teaching. **Dante**, well done in the project.

Thanks to all the people in MBW department for providing a good working environment. Especially thanks to **Neus Visa**, **Anders Nilsson** and **Ulrich Theopold** for useful advices and interesting discussions in IPS. Thanks to **Neus** for the guiding of PhD study too.

I am also grateful to a group of Chinese friends. And I am so lucky to have you around and enjoyed the time spent in Stockholm. **Kun Wang**, **Wei Si**, **Xiongzhuo Tang**, **Yunpo Zhao**, **Liqun Yao**, **Li Dang** and **Lidi Xu**, just to name a few, thanks for all the help. As most of you have already graduated, best wishes in future life.

Finally, my sincere gratitude goes to my family. My parents and my sister, thanks for giving me endless love and support. Great thanks to my husband and best friend, **Changrong**. Thank you for making my life like an adventure. It's really a more colorful world than I thought previously. You make everything feel possible. My daughter **Ziqi**, lovely and noisy, thanks for all the happiness you bring to me. Imagining life without you is impossible.

References

1. IAEA. Radiation, People and the Environment. 2004.
2. Eric J. Hall AJG. Radiobiology for the radiologist. Seventh ed: Lippincott Williams and Wilkins; 2012.
3. Gayle Woodside DK. Environmental, Safety, and Health Engineering 1997.
4. Charles M. UNSCEAR report 2000: sources and effects of ionizing radiation. United Nations Scientific Committee on the Effects of Atomic Radiation. J Radiol Prot. 2001;21(1):83-6.
5. Pouget JP. MSJ. General aspects of the cellular response to low- and high-LET radiation. European Journal of Nuclear Medicine. 2001;28(4):541-61.
6. Nikjoo H, Bolton CE, Watanabe R, Terrissol M, O'Neill P, Goodhead DT. Modelling of DNA damage induced by energetic electrons (100 eV to 100 keV). Radiat Prot Dosimetry. 2002;99(1-4):77-80.
7. Task Group on Radiation Quality Effects in Radiological Protection CoREICoRP. Relative biological effectiveness (RBE), quality factor (Q), and radiation weighting factor (w(R)). A report of the International Commission on Radiological Protection. Ann ICRP. 2003;33(4):1-117.
8. Harrison J, Day P. Radiation doses and risks from internal emitters. J Radiol Prot. 2008;28(2):137-59.
9. Laramore G.E. LJJ, Rockhill J.K., Komarnicky-Kocher L.T. Relative Biological Effectiveness (RBE). In: Brady LW, Yaeger TE, editors. Encyclopedia of Radiation Oncology: Springer, Berlin, Heidelberg; 2013.
10. Omar Desouky ND, Guangming Zhou. Targeted and non-targeted effects of ionizing radiation. Journal of Radiation Research and Applied Sciences. 2015;8(2):247-54.
11. Penny Jeggo ML. RADIATION-INDUCED DNA DAMAGE RESPONSES. Radiation Protection Dosimetry. 2007;122:124-7.
12. Cadet J DT, Douki T, Gasparutto D, Pouget J-P, Ravanat J-L, Sauvaigo S. Hydroxyl radicals and DNA base damage. Mutation Research. 1999;424:9-21.

13. Ward J. Radiation mutagenesis: the initial DNA lesions responsible. *Radiat Res.* 1995;142(3):362-8.
14. Mavragani IV, NZ, Souli MP., Aziz A., Newsheen S., Aziz K., Rogakou E., Georgakilas AG. Complex DNA Damage: A Route to Radiation-Induced Genomic Instability and Carcinogenesis. *Cancer.* 2017;18;9(7).
15. Semenenko VA SR. A Fast Monte Carlo Algorithm to Simulate the Spectrum of DNA Damages Formed by Ionizing Radiation. *Radiat Res.* 2004;161(4):451-7.
16. Nikjoo H ONP, Terrissol M, Goodhead DT. Quantitative modelling of DNA damage using Monte Carlo track structure method. *Radiat Environ Biophys.* 1999;38(1):31-8.
17. Terato H TR, Nakaarai Y, Nohara T, Doi Y, Iwai S, Hirayama R, Furusawa Y, Ide H. Quantitative analysis of isolated and clustered DNA damage induced by gamma-rays, carbon ion beams, and iron ion beams. *J Radiat Res.* 2008;49(2)(133-46).
18. Lindahl T BD. Repair of endogenous DNA damage: Cold Spring Harb Symp Quant Biol; 2000.
19. Chatterjee N, Walker GC. Mechanisms of DNA damage, repair, and mutagenesis. *Environ Mol Mutagen.* 2017;58(5):235-63.
20. Harper JW, Elledge SJ. The DNA damage response: ten years after. *Mol Cell.* 2007;28(5):739-45.
21. Zhou BB, Elledge SJ. The DNA damage response: putting checkpoints in perspective. *Nature.* 2000;408(6811):433-9.
22. Hegde ML, Izumi T, Mitra S. Oxidized base damage and single-strand break repair in mammalian genomes: role of disordered regions and posttranslational modifications in early enzymes. *Prog Mol Biol Transl Sci.* 2012;110:123-53.
23. Scharer OD. Nucleotide excision repair in eukaryotes. *Cold Spring Harb Perspect Biol.* 2013;5(10):a012609.
24. Santivasi WL, Xia F. Ionizing radiation-induced DNA damage, response, and repair. *Antioxid Redox Signal.* 2014;21(2):251-9.
25. Lieber MR. The mechanism of double-strand DNA break repair by the nonhomologous DNA end-joining pathway. *Annu Rev Biochem.* 2010;79:181-211.
26. Sonoda E, Hohegger H, Saberi A, Taniguchi Y, Takeda S. Differential usage of non-homologous end-joining and homologous recombination in double strand break repair. *DNA Repair (Amst).* 2006;5(9-10):1021-9.

27. Isono M, Niimi A, Oike T, Hagiwara Y, Sato H, Sekine R, et al. BRCA1 Directs the Repair Pathway to Homologous Recombination by Promoting 53BP1 Dephosphorylation. *Cell Rep.* 2017;18(2):520-32.
28. Ma Y, Lu H, Tippin B, Goodman MF, Shimazaki N, Koiwai O, et al. A biochemically defined system for mammalian nonhomologous DNA end joining. *Mol Cell.* 2004;16(5):701-13.
29. Chan DW, Chen BP, Prithivirajasingh S, Kurimasa A, Story MD, Qin J, et al. Autophosphorylation of the DNA-dependent protein kinase catalytic subunit is required for rejoining of DNA double-strand breaks. *Genes Dev.* 2002;16(18):2333-8.
30. Mimitou EP, Symington LS. DNA end resection: many nucleases make light work. *DNA Repair (Amst).* 2009;8(9):983-95.
31. Jasin M, Rothstein R. Repair of strand breaks by homologous recombination. *Cold Spring Harb Perspect Biol.* 2013;5(11):a012740.
32. Wang H, Perrault AR, Takeda Y, Qin W, Wang H, Iliakis G. Biochemical evidence for Ku-independent backup pathways of NHEJ. *Nucleic Acids Res.* 2003;31(18):5377-88.
33. McVey M, Lee SE. MMEJ repair of double-strand breaks (director's cut): deleted sequences and alternative endings. *Trends Genet.* 2008;24(11):529-38.
34. Shiloh Y, Ziv Y. The ATM protein: the importance of being active. *J Cell Biol.* 2012;198(3):273-5.
35. Guo Z, Kozlov S, Lavin MF, Person MD, Paull TT. ATM activation by oxidative stress. *Science.* 2010;330(6003):517-21.
36. Bakkenist CJ, Kastan MB. DNA damage activates ATM through intermolecular autophosphorylation and dimer dissociation. *Nature.* 2003;421(6922):499-506.
37. Czornak K, Chughtai S, Chrzanowska KH. Mystery of DNA repair: the role of the MRN complex and ATM kinase in DNA damage repair. *J Appl Genet.* 2008;49(4):383-96.
38. Uziel T, Lerenthal Y, Moyal L, Andegeko Y, Mittelman L, Shiloh Y. Requirement of the MRN complex for ATM activation by DNA damage. *EMBO J.* 2003;22(20):5612-21.
39. Lee JH, Paull TT. ATM activation by DNA double-strand breaks through the Mre11-Rad50-Nbs1 complex. *Science.* 2005;308(5721):551-4.
40. Lee JH, Paull TT. Activation and regulation of ATM kinase activity in response to DNA double-strand breaks. *Oncogene.* 2007;26(56):7741-8.
41. Zgheib O, Huyen Y, DiTullio RA, Jr., Snyder A, Venere M, Stavridi ES, et al. ATM signaling and 53BP1. *Radiother Oncol.* 2005;76(2):119-22.

42. Collis SJ, DeWeese TL, Jeggo PA, Parker AR. The life and death of DNA-PK. *Oncogene*. 2005;24(6):949-61.
43. Jackson SP, Bartek J. The DNA-damage response in human biology and disease. *Nature*. 2009;461(7267):1071-8.
44. Huen MS, Chen J. The DNA damage response pathways: at the crossroad of protein modifications. *Cell Res*. 2008;18(1):8-16.
45. Reinhardt HC, Schumacher B. The p53 network: cellular and systemic DNA damage responses in aging and cancer. *Trends Genet*. 2012;28(3):128-36.
46. Petitjean A, Mathe E, Kato S, Ishioka C, Tavtigian SV, Hainaut P, et al. Impact of mutant p53 functional properties on TP53 mutation patterns and tumor phenotype: lessons from recent developments in the IARC TP53 database. *Hum Mutat*. 2007;28(6):622-9.
47. Riley T, Sontag E, Chen P, Levine A. Transcriptional control of human p53-regulated genes. *Nat Rev Mol Cell Biol*. 2008;9(5):402-12.
48. Ford JM. Regulation of DNA damage recognition and nucleotide excision repair: another role for p53. *Mutat Res*. 2005;577(1-2):195-202.
49. Batchelor E, Loewer A, Lahav G. The ups and downs of p53: understanding protein dynamics in single cells. *Nat Rev Cancer*. 2009;9(5):371-7.
50. Knops K, Boldt S, Wolkenhauer O, Kriehuber R. Gene expression in low- and high-dose-irradiated human peripheral blood lymphocytes: possible applications for biodosimetry. *Radiat Res*. 2012;178(4):304-12.
51. Brengues M, Paap B, Bittner M, Amundson S, Seligmann B, Korn R, et al. Biodosimetry on small blood volume using gene expression assay. *Health Phys*. 2010;98(2):179-85.
52. Boldt S, Knops K, Kriehuber R, Wolkenhauer O. A frequency-based gene selection method to identify robust biomarkers for radiation dose prediction. *Int J Radiat Biol*. 2012;88(3):267-76.
53. Meador JA, Ghandhi SA, Amundson SA. p53-independent downregulation of histone gene expression in human cell lines by high- and low-let radiation. *Radiat Res*. 2011;175(6):689-99.
54. Turtoi A, Brown I, Schlager M, Schneeweiss FH. Gene expression profile of human lymphocytes exposed to (211)At alpha particles. *Radiat Res*. 2010;174(2):125-36.
55. Turtoi A, Schneeweiss FH. Effect of (211)At alpha-particle irradiation on expression of selected radiation responsive genes in human lymphocytes. *Int J Radiat Biol*. 2009;85(5):403-12.

56. Beer L, Seemann R, Ristl R, Ellinger A, Kasiri MM, Mitterbauer A, et al. High dose ionizing radiation regulates micro RNA and gene expression changes in human peripheral blood mononuclear cells. *BMC Genomics*. 2014;15:814.
57. Li S, Lu X, Feng JB, Tian M, Liu QJ. Identification and Validation of Candidate Radiation-responsive Genes for Human Biodosimetr. *Biomed Environ Sci*. 2017;30(11):834-40.
58. Hendry JH, Simon SL, Wojcik A, Sohrabi M, Burkart W, Cardis E, et al. Human exposure to high natural background radiation: what can it teach us about radiation risks? *J Radiol Prot*. 2009;29(2A):A29-42.
59. Bartlett DT. Radiation protection aspects of the cosmic radiation exposure of aircraft crew. *Radiat Prot Dosimetry*. 2004;109(4):349-55.
60. Forman JD, Yudelev M, Bolton S, Tekyi-Mensah S, Maughan R. Fast neutron irradiation for prostate cancer. *Cancer Metastasis Rev*. 2002;21(2):131-5.
61. Capala J, Stenstam BH, Skold K, Munck af Rosenschold P, Giusti V, Persson C, et al. Boron neutron capture therapy for glioblastoma multiforme: clinical studies in Sweden. *J Neurooncol*. 2003;62(1-2):135-44.
62. Staaf E. Cellular effects after exposure to mixed beams of ionizing radiation: Stockholm University.
63. Staaf E, Brehwens K, Haghdoost S, Nievaart S, Pachnerova-Brabcova K, Czub J, et al. Micronuclei in human peripheral blood lymphocytes exposed to mixed beams of X-rays and alpha particles. *Radiat Environ Biophys*. 2012;51(3):283-93.
64. Staaf E, Brehwens K, Haghdoost S, Czub J, Wojcik A. Gamma-H2AX foci in cells exposed to a mixed beam of X-rays and alpha particles. *Genome Integr*. 2012;3(1):8.
65. Staaf E, Deperas-Kaminska M, Brehwens K, Haghdoost S, Czub J, Wojcik A. Complex aberrations in lymphocytes exposed to mixed beams of (241)Am alpha particles and X-rays. *Mutat Res*. 2013;756(1-2):95-100.
66. Sax K, Enzmann EV. The Effect of Temperature on X-Ray Induced Chromosome Aberrations. *Proc Natl Acad Sci U S A*. 1939;25(8):397-405.
67. Sax K. Temperature Effects on X-Ray Induced Chromosome Aberrations. *Genetics*. 1947;32(1):75-8.
68. Elmroth K, Nygren J, Erkell LJ, Hultborn R. Effect of hypothermic irradiation of the growth characteristics of two human cell lines. *Anticancer Res*. 2000;20(5B):3429-33.

69. Bajerska A, Liniecki J. The influence of temperature at irradiation in vitro on the yield of chromosomal aberrations in peripheral blood lymphocytes. *Int J Radiat Biol Relat Stud Phys Chem Med.* 1969;16(5):483-93.
70. Gumrich K, Virsik-Peuckert RP, Harder D. Temperature and the formation of radiation-induced chromosome aberrations. I. The effect of irradiation temperature. *Int J Radiat Biol Relat Stud Phys Chem Med.* 1986;49(4):665-72.
71. Lisowska H, Wegierek-Ciuk A, Banasik-Nowak A, Braziewicz J, Wojewodzka M, Wojcik A, et al. The dose-response relationship for dicentric chromosomes and gamma-H2AX foci in human peripheral blood lymphocytes: influence of temperature during exposure and intra- and inter-individual variability of donors. *Int J Radiat Biol.* 2013;89(3):191-9.
72. Kempner ES, Haigler HT. The influence of low temperature on the radiation sensitivity of enzymes. *J Biol Chem.* 1982;257(22):13297-9.
73. Brzozowska K, Johannes C, Obe G, Hentschel R, Morand J, Moss R, et al. Effect of temperature during irradiation on the level of micronuclei in human peripheral blood lymphocytes exposed to X-rays and neutrons. *Int J Radiat Biol.* 2009;85(10):891-9.
74. Brehwens K, Staaf E, Haghdoost S, Gonzalez AJ, Wojcik A. Cytogenetic damage in cells exposed to ionizing radiation under conditions of a changing dose rate. *Radiat Res.* 2010;173(3):283-9.
75. Dang L, Lisowska H, Manesh SS, Sollazzo A, Deperas-Kaminska M, Staaf E, et al. Radioprotective effect of hypothermia on cells - a multiparametric approach to delineate the mechanisms. *Int J Radiat Biol.* 2012;88(7):507-14.
76. Elmroth K, Erkell LJ, Nygren J, Hultborn R. Radiation and hypothermia: changes in DNA supercoiling in human diploid fibroblasts. *Anticancer Res.* 1999;19(6B):5307-11.
77. Elmroth K, Nygren J, Stenerlow B, Hultborn R. Chromatin- and temperature-dependent modulation of radiation-induced double-strand breaks. *Int J Radiat Biol.* 2003;79(10):809-16.
78. Cheng L, Lisowska H, Sollazzo A, Wegierek-Ciuk A, Stepien K, Kuszewski T, et al. Modulation of radiation-induced cytogenetic damage in human peripheral blood lymphocytes by hypothermia. *Mutat Res Genet Toxicol Environ Mutagen.* 2015;793:96-100.
79. Brooks AL, Hoel DG, Preston RJ. The role of dose rate in radiation cancer risk: evaluating the effect of dose rate at the molecular, cellular and tissue levels using key events in critical pathways following exposure to low LET radiation. *Int J Radiat Biol.* 2016;92(8):405-26.

80. Hall EJ, Brenner DJ. The dose-rate effect revisited: radiobiological considerations of importance in radiotherapy. *Int J Radiat Oncol Biol Phys.* 1991;21(6):1403-14.
81. Mitchell CR, Folkard M, Joiner MC. Effects of exposure to low-dose-rate (60)co gamma rays on human tumor cells in vitro. *Radiat Res.* 2002;158(3):311-8.
82. Favaudon V, Caplier L, Monceau V, Pouzoulet F, Sayarath M, Fouillade C, et al. Ultrahigh dose-rate FLASH irradiation increases the differential response between normal and tumor tissue in mice. *Sci Transl Med.* 2014;6(245):245ra93.
83. Vozenin MC, De Fornel P, Petersson K, Favaudon V, Jaccard M, Germond JF, et al. The Advantage of FLASH Radiotherapy Confirmed in Mini-pig and Cat-cancer Patients. *Clin Cancer Res.* 2019;25(1):35-42.
84. Durante M, Brauer-Krisch E, Hill M. Faster and safer? FLASH ultra-high dose rate in radiotherapy. *Br J Radiol.* 2018;91(1082):20170628.
85. Ling CC, Gerweck LE, Zaider M, Yorke E. Dose-rate effects in external beam radiotherapy redux. *Radiother Oncol.* 2010;95(3):261-8.
86. IAEA. Cytogenetic dosimetry: applications in preparedness for and response to radiation emergencies. International Atomic Energy Agency, Vienna. 2011.
87. Ozasa K, Cullings HM, Ohishi W, Hida A, Grant EJ. Epidemiological studies of atomic bomb radiation at the Radiation Effects Research Foundation. *Int J Radiat Biol.* 2019:1-13.
88. Ruhm W, Azizova T, Bouffler S, Cullings HM, Grosche B, Little MP, et al. Typical doses and dose rates in studies pertinent to radiation risk inference at low doses and low dose rates. *J Radiat Res.* 2018;59(suppl_2):ii1-ii10.
89. Ponten J, Saksela E. Two established in vitro cell lines from human mesenchymal tumours. *Int J Cancer.* 1967;2(5):434-47.
90. Bayani J, Zielenska M, Pandita A, Al-Romaih K, Karaskova J, Harrison K, et al. Spectral karyotyping identifies recurrent complex rearrangements of chromosomes 8, 17, and 20 in osteosarcomas. *Genes Chromosomes Cancer.* 2003;36(1):7-16.
91. Isfort RJ, Cody DB, Lovell G, Doersen CJ. Analysis of oncogenes, tumor suppressor genes, autocrine growth-factor production, and differentiation state of human osteosarcoma cell lines. *Mol Carcinog.* 1995;14(3):170-8.

92. Liu Z, Liu Q, Xu B, Wu J, Guo C, Zhu F, et al. Berberine induces p53-dependent cell cycle arrest and apoptosis of human osteosarcoma cells by inflicting DNA damage. *Mutat Res.* 2009;662(1-2):75-83.
93. Bekker-Jensen S, Lukas C, Melander F, Bartek J, Lukas J. Dynamic assembly and sustained retention of 53BP1 at the sites of DNA damage are controlled by Mdc1/NFBD1. *J Cell Biol.* 2005;170(2):201-11.
94. Staaf E, Brehwens K, Haghdoost S, Pachnerova-Brabcova K, Czub J, Braziewicz J, et al. Characterisation of a setup for mixed beam exposures of cells to 241Am alpha particles and X-rays. *Radiat Prot Dosimetry.* 2012;151(3):570-9.
95. Mahmood T, Yang PC. Western blot: technique, theory, and trouble shooting. *N Am J Med Sci.* 2012;4(9):429-34.
96. Banda M, Bommineni A, Thomas RA, Luckinbill LS, Tucker JD. Evaluation and validation of housekeeping genes in response to ionizing radiation and chemical exposure for normalizing RNA expression in real-time PCR. *Mutat Res.* 2008;649(1-2):126-34.
97. Olive PL. The comet assay. An overview of techniques. *Methods Mol Biol.* 2002;203:179-94.
98. Collins AR. The comet assay for DNA damage and repair: principles, applications, and limitations. *Mol Biotechnol.* 2004;26(3):249-61.
99. Ostling O, Johanson KJ. Microelectrophoretic study of radiation-induced DNA damages in individual mammalian cells. *Biochem Biophys Res Commun.* 1984;123(1):291-8.
100. Singh NP, McCoy MT, Tice RR, Schneider EL. A simple technique for quantitation of low levels of DNA damage in individual cells. *Exp Cell Res.* 1988;175(1):184-91.
101. Burlinson B, Tice RR, Speit G, Agurell E, Brendler-Schwaab SY, Collins AR, et al. Fourth International Workgroup on Genotoxicity testing: results of the in vivo Comet assay workgroup. *Mutat Res.* 2007;627(1):31-5.
102. Holt SM, Georgakilas AG. Detection of complex DNA damage in gamma-irradiated acute lymphoblastic leukemia Pre-b NALM-6 cells. *Radiat Res.* 2007;168(5):527-34.
103. Georgakilas AG, Holt SM, Hair JM, Loftin CW. Measurement of oxidatively-induced clustered DNA lesions using a novel adaptation of single cell gel electrophoresis (comet assay). *Curr Protoc Cell Biol.* 2010;Chapter 6:Unit 6 11.
104. Fenech M. The in vitro micronucleus technique. *Mutat Res.* 2000;455(1-2):81-95.

105. Fenech M. The micronucleus assay determination of chromosomal level DNA damage. *Methods Mol Biol.* 2008;410:185-216.
106. Higuchi R, Fockler C, Dollinger G, Watson R. Kinetic PCR analysis: real-time monitoring of DNA amplification reactions. *Biotechnology (N Y).* 1993;11(9):1026-30.
107. Wong ML, Medrano JF. Real-time PCR for mRNA quantitation. *Biotechniques.* 2005;39(1):75-85.
108. Spanakis E. Problems related to the interpretation of autoradiographic data on gene expression using common constitutive transcripts as controls. *Nucleic Acids Res.* 1993;21(16):3809-19.
109. Banerjee S, An S, Makino S. Specific cleavage of 28S ribosomal RNA in murine coronavirus-infected cells. *Adv Exp Med Biol.* 2001;494:621-6.
110. Kato H, Sandberg AA. Chromosome pulverization in human binucleate cells following colcemid treatment. *J Cell Biol.* 1967;34(1):35-45.
111. Kato H, Sandberg AA. Chromosome pulverization in human cells with micronuclei. *J Natl Cancer Inst.* 1968;40(1):165-79.
112. Mullinger AM, Johnson RT. Units of chromosome replication and packing. *J Cell Sci.* 1983;64:179-93.
113. Hittelman WN, Pollard M. Visualization of chromatin events associated with repair of ultraviolet light-induced damage by premature chromosome condensation. *Carcinogenesis.* 1984;5(10):1277-85.
114. Gotoh EA, Y. Kosaka H. Inhibition of protein serine/threonine phosphatases directly induces premature chromosome condensation in mammalian somatic cells. *Biomedical Research.* 1995;16(1):63-8.
115. Balakrishnan S, Shirsath K, Bhat N, Anjaria K. Biodosimetry for high dose accidental exposures by drug induced premature chromosome condensation (PCC) assay. *Mutat Res.* 2010;699(1-2):11-6.
116. Steel GG, Peckham MJ. Exploitable mechanisms in combined radiotherapy-chemotherapy: the concept of additivity. *Int J Radiat Oncol Biol Phys.* 1979;5(1):85-91.
117. Streffer C, Muller WU. Dose-effect relationships and general mechanisms of combined exposures. *Int J Radiat Biol Relat Stud Phys Chem Med.* 1987;51(6):961-9.
118. Sage E, Shikazono N. Radiation-induced clustered DNA lesions: Repair and mutagenesis. *Free Radic Biol Med.* 2017;107:125-35.
119. Rall M, Kraft D, Volcic M, Cucu A, Nasonova E, Taucher-Scholz G, et al. Impact of Charged Particle Exposure on Homologous DNA Double-Strand Break Repair in Human Blood-Derived Cells. *Front Oncol.* 2015;5:250.

120. Costes SV, Boissiere A, Ravani S, Romano R, Parvin B, Barcellos-Hoff MH. Imaging features that discriminate between foci induced by high- and low-LET radiation in human fibroblasts. *Radiat Res.* 2006;165(5):505-15.
121. Jakob B, Rudolph JH, Gueven N, Lavin MF, Taucher-Scholz G. Live cell imaging of heavy-ion-induced radiation responses by beamline microscopy. *Radiat Res.* 2005;163(6):681-90.
122. Jakob B, Splinter J, Taucher-Scholz G. Positional stability of damaged chromatin domains along radiation tracks in mammalian cells. *Radiat Res.* 2009;171(4):405-18.
123. Lisowska H, Brehwens K, Zolzer F, Wegierek-Ciuk A, Czub J, Lankoff A, et al. Effect of hypothermia on radiation-induced micronuclei and delay of cell cycle progression in TK6 cells. *Int J Radiat Biol.* 2014;90(4):318-24.
124. Johannes C, Dixius A, Pust M, Hentschel R, Buraczewska I, Staaf E, et al. The yield of radiation-induced micronuclei in early and late-arising binucleated cells depends on radiation quality. *Mutat Res.* 2010;701(1):80-5.
125. Mill AJ, Wells J, Hall SC, Butler A. Micronucleus induction in human lymphocytes: comparative effects of X rays, alpha particles, beta particles and neutrons and implications for biological dosimetry. *Radiat Res.* 1996;145(5):575-85.
126. Depuydt J, Baeyens A, Barnard S, Beinke C, Benedek A, Beukes P, et al. RENEB intercomparison exercises analyzing micronuclei (Cytokinesis-block Micronucleus Assay). *Int J Radiat Biol.* 2017;93(1):36-47.
127. Macaeva E, Saeys Y, Tabury K, Janssen A, Michaux A, Benotmane MA, et al. Radiation-induced alternative transcription and splicing events and their applicability to practical biodosimetry. *Sci Rep.* 2016;6:19251.